AD-A174 668 LOCAL-GLOBAL INTERACTIONS IN THE TRANSIENT RESPONSE OF 1/1
LATTICE-TRUSS PLAT..(U) LOCKHEED MISSILES AND SPACE CO
INC PALO ALTO CA PALO ALTO RES..
UNCLASSIFIED M E REGELBRUGGE ET AL. AUG 84 LMSC-D878939 F/G 22/2 NL

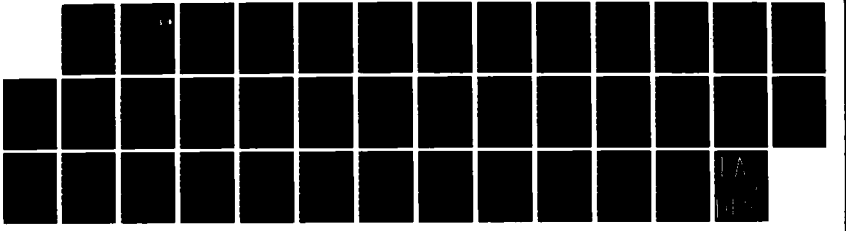

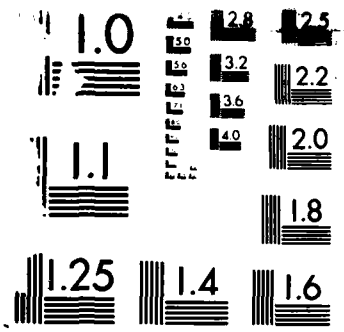

AFOSR-TR- 86-0452

LMSC-D878939

Local-Global Interactions in the Transient Response of Lattice-Truss Plates

M. E. Regelbrugge and K. C. Park
Applied Mechanics Laboratory
Lockheed Palo Alto Research Laboratory
Palo Alto, Califorina

February 1984/Revised August 1984

Abstract

The transient response of lattice-truss plates is studied with emphasis on how the individual lattice members dynamic characteristics influence the transient response characteristics. When the lattice members are modeled as bars, the transient responses are dominated by the low-frequency components that correspond to the continuum thick plate case. However, when the lattice members are modeled as slender beams to be more realistic, the dynamic characteristics of the individual lattice members significantly influence the global transient response. The level of influence increases as the member slenderness ratio increases. The results underscore the importance of local high-wave member modes that must be treated satisfactorily both in passive and active control of large lattice-truss space structures.

Presented at the 24th Structures, Materials and Dynamics Conference, 14-16 May 1984, Palm Springs, Ca. Paper No. AIAA-84-0945-CP.

SECURITY CLASSIFICATION OF THIS PAGE (When Data Entered)

REPORT DOCUMENTATION PAGE		READ INSTRUCTIONS BEFORE COMPLETING FORM
1. REPORT NUMBER AFOSR-TR- 86-0452	2. GOVT ACCESSION NO.	3. RECIPIENT'S CATALOG NUMBER
4. TITLE (and Subtitle) Local-Global Interactions in the Transient Response of Lattice-Truss Plates		5. TYPE OF REPORT & PERIOD COVERED Annual 6. PERFORMING ORG. REPORT NUMBER LMSC-D878939
7. AUTHOR(s) M.E. Regelbrugge and K.C.Park		8. CONTRACT OR GRANT NUMBER(s) F49620-83-C-0018
9. PERFORMING ORGANIZATION NAME AND ADDRESS Lockheed Palo Alto Research Laboratory 3251 Porter Drive Palo Alto, CA 94304		10. PROGRAM ELEMENT, PROJECT, TASK AREA & WORK UNIT NUMBERS 61102F 2302/B1
11. CONTROLLING OFFICE NAME AND ADDRESS Air Force Office of Scientific Research NM		12. REPORT DATE February, 1984 13. NUMBER OF PAGES 36
14. MONITORING AGENCY NAME & ADDRESS(if different from Controlling Office) Building 410 Bolling AFB DC 20332-6448		15. SECURITY CLASS. (of this report) Unclassified 15a. DECLASSIFICATION/DOWNGRADING SCHEDULE

16. DISTRIBUTION STATEMENT (of this Report)

Approved for public release,
distribution unlimited

17. DISTRIBUTION STATEMENT (of the abstract entered in Block 20, if different from Report)

18. SUPPLEMENTARY NOTES

19. KEY WORDS (Continue on reverse side if necessary and identify by block number)

Dynamics, Transient Response, Large Space Structures, Lattice Space Structures

20. ABSTRACT (Continue on reverse side if necessary and identify by block number)

The transient response of lattice-truss plates is studied with emphasis on how the individual lattice members dynamic characteristics influence the transient response characteristics. When the lattice members are modeled as bars, the transient responses are dominated by the low-frequency components that correspond to the continuum thick plate case. However, when the lattice members are modeled as slender beams to be more realistic, the dynamic characteristics of the individual lattice members significantly influence the global transient

(continued - over)

DD FORM 1 JAN 73 1473 EDITION OF 1 NOV 65 IS OBSOLETE

Unclassified

SECURITY CLASSIFICATION OF THIS PAGE (When Data Entered)

(Block 20, continued)

response. The level of influence increases as the member slenderness ratio increases. The results underscore the importance of local high-wave member modes that must be treated satisfactorily both in passive and active control of large lattice-truss space structures.

1. Introduction

Space structures to be deployed in the future consist largely of lattice construction. The control of the inevitable vibrations in the structure to meet mission performance requirements presents a challenge to both the structural and control engineers. The prevailing approaches for the control of vibrations are based on the assumption that the vibrations are dominated by the low-frequency, long-wave modes which are often referred to as global modes. As such, strategies for active vibration control, passive damping devices, and representation of flexibility in multi-body dynamics accommodate largely the low-frequency global frequencies and their mode shapes. For large space structures made of slender lattice members, e.g., their slenderness ratio ranging from 800 to 1000, however, this assumption may not hold; it may be necessary to account for the so-called high-wave mode shapes whose frequencies are nonetheless comparable with those of the long-wave global modes.

It was shown in previous studies [1-3] that when the lattice is modeled as truss, the global modes dominate, justifying the prevailing assumption. As the member slenderness ratio increases so that the member model must account for the beam bending and cable phenomena, however, the frequencies of the individual lattice member modes gradually start to decrease; the frequency gap between the global modes and the individual lattice member modes become narrower. In fact, when the lattice structures are optimized, it is conceivable that the global mode frequencies would be practically the same as those of the individual local member modes. This phenomenon is not unique to vibrations of the large space lattice structures. In buckling of optimized thin shells, the long-wave global buckling loads become quite close to those of short-wave buckling modes; in fact, an optimum design criterion for thin shells is often to have both global and local buckling occurring at the same load.

The objectives of the present paper are: (1) to verify the significant role of the short-wave local modes in the overall transient response of the large lattice-truss space structures; (2) to study the manner by which the energy associated with the disturbances propagates and how the local truss members influence the spatial energy distribution patterns throughout the response period; and (3) to explore means to utilize the closely coupled local-global interactions to design advantages. To this end, the paper is organized as follows.

Section 2 describes the model truss plate which will be used for the present transient response analysis and presents the global vibration modes and the associated frequencies when the truss members are modeled as bars. It is shown that the global vibration modes and their frequencies can be adequately modeled by treating the truss members as bars. The truss plate model for the subsequent transient response analysis is presented in Section 3, in which the truss members are modelled as beams in order to account for the effect of beam bending behavior on the local as well as the global transient responses under implusive loads. To assess the influence of the member slenderness ratios on the local-global interactions, three slenderness ratios are considered

s = 250, 429, and 600.

The linear transient analysis results of the model truss plate are presented in Section 4. In order to generalize the results independent of the generic truss model plate, a measure of *specific strain energy* is proposed and used extensively for evaluating the analysis results. The results show that the responses at the truss joints consist of significant high-frequency components that prevail throughout the transient response period, thus reinforcing the importance of including the individual member characteristics into the discrete model for realistic dynamic analyses. In addition, the responses at interior points of the truss members demonstrate that the truss member deformation is strongly influenced by the member bending deformation modes and this influence increases with the increase in the member slenderness ratio.

Fourier analysis of the linear transient analysis results are described in Section 5. It is shown that bending deformations of the individual truss members occur with high amplitudes and that they share a significant portion of the system energy. This share increases with an increase in the member slenderness ratio. Further, the Fourier analysis shows that high-frequency components are significant constituents of the response, and that they are a mixture of high global modes.

The energy propagation and its spatial distribution patterns are studied in Section 6. A study of single tetrahedron cell with various lattice stiffness changes demonstrates that, such stiffness variations among the truss members, even though they bring about relatively small perturbations in the global vibration frequencies and mode shapes, do redistribute drastically the system energy share of the individual truss members. Furthermore, the energy distribution patterns are strongly influenced by the changes in stiffness of the core members relative to the surface members.

Major results and the implications of the present findings on the passive and active vibration control strategies are summarized in Section 7. Future study areas extendig the present study into more realistic nonlinear modelling are also outlined.

2. Vibrations of Truss-Model Lattice Plate

In order to gain insight into the overall characteristics of the lattice truss plate under dynamic loads, free-free vibrations of the lattice plate whose lattice members are modeled as truss bars are first studied. It is noted that the resulting vibration modes correspond to the free vibrations of a thick plate. Hence, depending upon the geometry of the plate and member sizes, transverse shear deformation can play an important role. Figure 1 illustrates the truss plate model which consists of 1113 truss members whose slenderness ratio is chosen to be 250. The dimensions of the resulting plate are thus 10-by-12 tetrahedron cells.

Modeling of the classical hinged truss joint was accomplished by suppressing all rotational freedoms at truss joints and defining an extremely small rotational stiffness for the engineering beam finite elements. In this manner, the computational size and

complexity of the model was reduced to a manageable level without violating the truss assumption. Member properties were modified to provide a linearized approximation of imperfection sensitivity of a nonlinear beam member by reducing the elastic modulus from an hypothetical material ($E = 2.5 \times 10^6$psi) according to the formula

$$\bar{E} = \kappa E, \qquad \kappa = \frac{1}{(1 + .5(\alpha s)^2)} \tag{1}$$

where $\bar{E}$ is an effective material elastic modulus, E is the actual material elastic modulus, α is a nondimensional imperfection parameter, and s is the member slenderness ratio. For the present analysis purpose, it was decided that member frequencies should not change due to this modulus modification accounting for imperfection sensitivity. This was accomplished by also scaling the material density by the factor κ. This modification produces, in effect, a lower bound on global vibration frequencies without changing the linear character of the vibration analysis. Further explanation and justification of this formula appears in the Appendix.

The vibration nodal lines for the first four global modes are shown in Figure 2. Note that the first mode shape is dominated by shear deformation of the truss core, analogous to the response of a continuum thick plate. The higher modes are mixtures of thin plate bending and core shear deformations. In the highest modes, the bending wavelength is so short that considerable core shear deformation is produced, confirming the analogy to the continuum thick plate. It is interesting to note that the higher the frequencies become, the more closely clustered they become; in parallel with the relative difference in wave numbers. Thus, the free vibration spectrum for these structures is quite dense, especially in the higher frequencies.

These free vibration results indicate that global modal characteristics of lattice truss plates can be effectively modeled using the truss bar model of lattice members. One implication of this result is that the long-wave global modes are associated with extensional member deformations only. Therefore, continuum models based solely on member extensional stiffness properties [4-6] may be used to model truss plate global vibrations.

The above observations on the vibration characteristics of lattice plates whose members are modeled as truss bars play an important role in interpreting the transient response analysis results which will be described in the following sections.

3. Truss Plate Model for Transient Response Analysis

An important difference between the global truss vibration and transient response analysis arises in the modeling of truss members as actual slender beams. This means that although the structure is still modeled as a truss from the *static* point of view, the members are now able to deform in realistic *dynamic* modes. This approach requires greater detail in the modeling of individual members.

To model truss members as slender beams, two Hermitian cubic beam finite elements are used for each member, permitting adequate representation of member deflections up to the third bending mode of each truss member. The members are connected to one another by specifying coincident translational degrees of freedom at each member joint. Rotational degrees of freedom are thus local to a single parent member and did not influence adjacent members. This scheme is equivalent to constructing a pure hinge or *ball* joint at truss connections.

The model employed for the transient response analysis is identical in physical size and topology to that used for the truss-model vibration analyses. Since the members could respond to bending deformations, rotational degrees of freedom are admitted and member bending rigidity is set according to the desired member slenderness ratio. Table 1 lists the member physical properties adopted for the model. Note that the masses and axial stiffnesses are identical for all members regardless of slenderness ratio.

Slenderness Ratio s	*Cross-section Area* $A(in^2)$	*Bending Inertias* $I_{yy}, I_{zz}(in^4)$	*Effective Modulus* $\bar{E}(10^6 psi)$	*Effective Density* $\bar{\rho}(lb - sec^2/in^4)$
250	.30787	.07543	.12177	1.261×10^{-5}
429	.30787	.02408	.12177	1.261×10^{-5}
600	.30787	.01231	.12177	1.261×10^{-5}

Table 1. Truss Member Physical and Mechanical Properties.

Figure 3 shows the impulsive loads applied to the plate model such that the response is dictated by the first global truss mode ($f_{\lambda_1} = 2.9$ Hz.), or nearly by the second truss mode ($f_{\lambda_2} = 4.2$ Hz.). For these reasons, the loadings are hereafter referred to as *first mode excitation* and *second mode excitation*, respectively.

The central difference explicit time integration scheme has been used to integrate the resulting equations of motion because it is robust, accurate, and easily implemented [7,8]. In fact, the size of the problem (14,000 degrees of freedom) and the nature of member connectivity are such that data storage requirements for assembled, profiled, system matrices make an implicit scheme extremely costly under the computing environment, namely, VAX 11/780. The explicit scheme has therefore been implemented in conjunction with an element-by-element force calculation routine which precludes the need for assembling system matrices. The time increment is determined so as not

to exceed the stability limit of the discrete beam element according to the Courant criterion [9].

4. Linear Transient Analysis Results

Three interpretive tools have been employed to gain insight into transient response characteristics of lattice plates: deflection time histories, Fourier spectral analysis of time history data, and contour plotting of element strain energies at selected timesteps. The first two techniques are common to most transient response analysis as they provide information about the magnitudes, time variations, and modal content of observable physical displacements. The third technique, contouring of element strain energies, has become available only recently with the advent of high-resolution color graphics display devices. Its primary advantage is the capability to represent a complex spatial distribution of deformation energy in a single, easily comprehended display of the model structure.

In the computations of element strain energy, it is desirable both to eliminate any influence due to member property scaling (as defined in Eq. 1) and to obtain a realistic idea of the relative amount of *deformation* in a member at any given point in time. The former consideration eliminates any bias which the scaling process may introduce, while the latter can provide a guide as to which members, or groups of members, may be likely candidates for application of energy dissipation devices, as the effectiveness of these devices is generally commensurate with the amount of deformation the members to which they are attached undergo.

Accordingly, the measure of strain energy is nondimensionalized by the members' axial stiffness and length. This measure is refferred to as *specific strain energy* ($\bar{U}$) and is given by the following relation for linear members of constant cross-section:

$$\bar{U} = \frac{1}{2l}\left(\int_0^l \epsilon_x^2 dx + \frac{I}{A}\int_0^l (\kappa_y^2 + \kappa_z^2) dx\right) \tag{2}$$

All of the energy contour plots appearing in this report and all member energy data refer to member *specific* energy.

Truss plate models composed of members of slenderness ratios 250, 429, and 600 have been used in linear transient response analyses with the first global mode excitation. The response of the truss plate of $s = 250$ was also simulated under excitation corresponding to the second global mode. However, because of excessive data collected from these simulations, only part of the most relevant results are summarized in this paper.

Figure 4 shows the lower surface of the truss plate containing the spatial joints $(A - E)$ where displacement histories are sampled. Due to the symmetry of deflection patterns in the free-free truss, only joints in one quarter of the structure need be sampled. All of the degrees of freedom sampled correspond to translational motion out of the plane of the truss plate.

4.1 Displacement Time History at Truss Joints

For the first mode excitation case, the observed transient responses closely resemble the first global vibration mode. For example, the deflections at joint E are very small when compared with responses at the other joints marked in Fig. 4 as it is located quite close to the nodal line of the first truss vibration mode. For the second mode excitation, however, the transient response deviates appreciably from the second truss vibration mode since the locations of impulse loading for this case are only approximate. Thus, the loading has the effect of exciting additional truss modes although the first truss mode is not excited by second mode excitations.

Figures 5 through 7 illustrate displacement time histories at joints A, B, and D, respectively for the case of $s = 250$ subjected to the first mode excitation. Note that these histories are characterized by the response components that require a relatively short time (50 - 75 % of the first mode period) before they develop into the first global truss mode. Moreover, the exhibition of higher frequency components of sizeable amplitude continues throughout the response. This is particularly evident in the response history at joint B (Fig. 6), where higher frequency components respond with amplitudes well over half that of the fundamental truss mode. Figures 8 through 10 show response histories at joints A, E, and C, respectively, for the case of $s = 250$ under the second mode excitation. As with first mode excitation, high frequency components are induced at significantly large amplitudes. Also, the second mode excitation responses are in fact more complex than those for the first mode excitation.

The foregoing analysis results indicate that the transient response components consist not only of the global vibration modes of the truss plate but also of vibrations in a wide frequency spectrum. In addition, the apparent magnitudes of high frequency components change with member slenderness ratio. Figures 11 and 12 show the displacement response histories at joint A for the plates made of members of $s = 450$ and $s = 600$, respectively. Note that the high frequency components diminish as the member slenderness ratio increases. Another difference due to member slenderness ratio is the observed global mode period. Measurements of the three global mode periods for plates made of members of $s = 250, 429$, and 600 yield values of .34 sec., .21 sec. and .24 sec., respectively. Note that the period associated with the frequency listed for the first truss mode is .33 sec. from Table 1. Thus, the variation of global mode period with member slenderness ratio is as much as 36 percent, a sizeable variation.

As the member slenderness ratio is of direct influence only on individual member bending dynamics, this trend can be further characterized by examining the transient dynamics of individual members, which are discussed in the following section.

4.2 Transient Response at Interior of Truss Member

Examination of responses at interior points of the truss members rather than at truss joints can demonstrate the dynamic behavior of the individual members most clearly. Figure 13 illustrates the deflection history at the point A1 (Fig. 4) for the

truss plate of $s = 429$. Note the smoothness and regularity of this member response. The primary frequency component of this response is found to be that of the member fundamental bending mode ($f_{1bending} = 3.0$ Hz.). In fact, examinations of deflections at the other member centers show that the member interior deflections are dominated by bending oscillations. Moreover, the interior deflection amplitudes generally decrease as slenderness ratio is lowered, or, equivalently, as bending frequency is increased. An important effect of the local member bending dynamics on global vibrations is to shift the global periods of oscillation. As shown, in Section 4.1, the fundamental period may shorten by over one-third depending on the truss member slenderness ratio. Periods for the fundamental beam bending mode of each individual truss member are .19 sec., .33 sec., and .47 sec. for the cases of $s = 250$, $s = 429$, and $s = 600$, respectively.

As the global mode frequency is related through Rayleigh's Quotient to the square root of the ratio of the deformation (strain) energy to the kinetic energy, an increase in frequency would accompany an increase in the deformation energy relative to the kinetic energy. An increase in the apparent global truss mode frequency is thus an indication of the deformation energy contained in local member modes. Since the member bending mode periods are longer than the global period in the two higher slenderness ratio cases, the increase in the total kinetic energy due to member flexure is less than the corresponding increase in the deformation energy. Consequently, an increase in the global mode frequency is observed. The magnitude of this increase is greatest for the case of $s = 429$ as the member bending and global mode frequencies are closer in this case than in the other cases studied.

5. Fourier Analysis of Linear Transient Response Results

The foregoing evaluations of time histories at lattice joints and at interior points of truss members have provided insight into the spatial distributions of system energy and the manner of the energy propagation. A Fourier analysis can augument insight into the local-global intraction phenomena by pinpointing the dominant components of the response and by providing an overall view of spatial variations of response constitution.

A response history can be decomposed into

$$q(t) = \sum_{i=1}^{\infty} A_i \sin\ \omega_i t \tag{3}$$

where ω_i are the discrete modal frequencies. For steady-state responses, A_i are constants, whereas for transient (unsteady) responses, A_i may vary with time. In addition, in nonlinear transient cases, ω_i may also vary with time. In the steady-state, the Fourier amplitudes A_i in Eq. (4) are given by

$$A_i = \frac{2}{N+1} \sum_{j=1}^{N} q(t_j) \sin\ \frac{i\pi\Delta t}{T} \tag{4}$$

where N discrete response data $q(t_j)$ are provided over the interval ($t_0 < t \leq T$, and $t_j = j\Delta t$), and A_i are the amplitudes that correspond to the i^{th} angular frequency. For sampling rates used in the present analysis, the maximum frequency is in excess of 160 $Hz.$, which provides a spectrum capable of adequately representing response components at all frequencies of interest, i.e., $\omega_i \leq 30$ Hz.

For the linear case with no damping, the variation of A_i with time in transient response arises from a truncation of the displacement history data over very small time intervals. In particular, components whose frequency is of the order of $\frac{1}{2(T-t_0)}$ or less are not adequately represented by the decomposition described in Eq. (4). In the presence of significant high-frequency components, many sampling points must be introduced in order to provide accurate estimates of the amplitudes of the low frequency components relative to the high frequency components. For the present studies, the lowest frequencies of interest (~ 2 Hz.) can be adequately represented over time intervals greater than .25-.30 sec., however, due to a low data sampling rate, a time interval of $0 < t < 1.2$ sec. was chosen.

In practice, only the *relative* amplitudes of the various frequency components are of interest, since the response varies linearly with excitation in the present linear cases. Thus, A_i are normalized linearly such that the greatest amplitude is scaled to be unity.

Figures 14, 15 and 16 show the response spectra of $s = 250$, $s = 429$, and and $s = 600$ plates at truss joint A (Fig. 4) for the interval ($0 < t < 1.2$ sec.). Note that the lowest frequency peak in Fig. 14 corresponds to the first global truss plate mode, whereas the lowest frequency peaks in Figs. 15 and 16 represent the member fundamental bending mode. Thus, while the member bending motion is hardly noticed in the case of $s = 250$, the member dynamics are quite influential at higher slenderness ratios, especially in the case of $s = 429$ where the observed amplitude of member motion is about 40% of the global mode amplitude.

Figures 17 and 18 show Fourier spectra at the center of member A1 (Fig. 4) for the cases of $s = 250$ and $s = 429$. The components appearing in the $s = 250$ spectrum are the same global vibrations noticed at the truss joints. However, in the case of $s = 429$, the component associated with the member bending motion dominates the response. The latter situation is also the case for the plate of $s = 600$. Thus, the greater the flexibility of the members is, the greater their response influences, by way of bending vibrations, the global transient motion.

Figures 14 through 16 also show significant vibrations around $17 \sim 19$ Hz. Close examinations of the spectra reveal the predominant high frequency components to be at 18.8 Hz. for the low slenderness ratio truss ($s = 250$) and at 17.7 Hz. for the highest slenderness ratio truss ($s = 600$). The intensity of the 18.8 Hz. component is roughly 40% that of the first truss mode motion in the case of $s = 250$. In the higher slenderness ratio trusses, this ratio is roughly 50% ($s = 429$) and around 30% ($s = 600$). Thus, the influence of the high frequency component in global transient responses is quite significant.

It is interesting to note that the high frequencies do not change appreciably with slenderness ratio. As such, they must be manifestations of higher global truss modes. Modes were found in the studies described in Section 2 at 17.68 Hz. and at 18.99 Hz. which, when superposed with the first global mode, produce the vertical motions which are observed in the truss responses. These two modes are shown in Figures 19(a) and (b), and the superposition of these modes with the first mode is shown in Figure 19(c). Since the motion exhibited in Fig. 19(c) is apparent in *all* first mode excitation cases to some degree and not in the second mode excitation case, it may be assumed that this motion results from effects of truss geometry and loading.

Another noteworthy aspect to be considered when examining the Fourier spectra is the physical location of a given point relative to that of the excited global vibration nodal lines. For a point located *on* the nodal line, the global mode frequency will not appear in the Fourier spectrum. Only vibration frequencies associated with other motions will be discernable. Conversely, for a point located *away from* the nodal lines, the limiting case being a point on an antinode line, the global frequency would be expected to be the dominant constituent of the spectrum. An interesting example is the response at joint B, which lies on antinode lines of both the first truss mode and the higher frequency mode. Along this antinode, the deflections corresponding to the first global truss mode diminish with proximity to the center of the truss plate, but the high frequency modal amplitudes vary little from their maximum values. Thus, the response at joints such as B exhibits the relative maximum observable amplitude of motion at the higher frequency. This is illustrated in Figures 20 and 21, which show response spectra at joint B for the $s = 429$ and $s = 600$ cases, respectively. Comparison of the high-frequency amplitudes in these figures with those in Figs. 15 and 16 clearly show the relative increase in influence of the high-frequency motions near the center of the truss plate.

Three major differences in truss dynamic behavior due to member slenderness are evident. First, as the member slenderness ratio is increased, the amplitude of the high frequency ($17 - 19$ Hz.) motion is changed, as noted previously from response time histories. Fourier spectra show that the amplitudes of the the $17 - 19$ Hz. response components at joint B reach about 57%, 68%, and 38% of the dominant first mode response for the cases of $s = 250$, $s = 429$, $s = 600$, respectively. In general, truss member motions are combinations of bending, rigid translations, and rigid rotations. Additionally, high frequency components are almost totally absent from the member translational motions, regardless of member slenderness ratio. Therefore, the high frequency component so noticeable in truss joint responses is primarily due to the rigid rotations of the truss surface members. Fourier spectra of vertical displacement histories of the core members, however, exhibit these higher frequency components as rigid vertical translations.

Second, an increase in the member slenderness may remove certain components from the transient response. For example, the response component of 6.2 Hz. exhibited

for the case of $s = 250$ is conspicuously absent in spectra taken from both cases of $s = 429$ and $s = 600$. It is of interest to note that the case of $s = 250$ is the only one in which the member fundamemtal bending frequency (5.15 Hz.) is *above* the first observed global truss mode frequency (2.94 Hz.), suggesting that the period of individual member bending oscillation, in concert with the time-rate of vibration energy transfer among members, is such that the response component of 6.2 Hz. is excited only in trusses composed of members of sufficiently low slenderness. Energy transfer among members in the higher slenderness cases occurs at a much slower rate, due to the lower member frequencies, with the consequence that only the first global truss mode is excited.

Third, influence of the member bending motions increases with the member slenderness. As shown in Fig. 18, two components are predominant, with local beam bending accounting for roughly twice the level of the first global truss mode. In the case where the member bending frequency is very close to the global truss mode frequency, the effect of member motions is visible even at truss joints, as shown for the cases of $s = 429$ and $s = 600$.

These results underscore the significant role of modes other than the global truss modes (e.g., the locam member modes) in the transient dynamic response of lattice truss plates and point to the potential utility of variations of the member slenderness in modifying global transient vibrations. In addition, the presence of large amplitudes exhibited in member bending vibrations may be exploited by extracting energy associated with these motions before it is transferred to the global truss modes. Further, since the response to high frequency modes is noticeable throughout the truss, even at joints located exactly on the global mode nodal lines, high frequency components must be considered in any active or passive vibration dissipation scheme.

6. Spatial Energy Distribution and Propagation Under Transient Loads.

So far, attention has been concentrated on the time histories and their component Fourier spectra for a truss plate subjected to impulsive loadings. Both the time histories and their Fourier spectra provide valuable information as to deformation levels and the associated frequency contents for preliminary design considerations. In this section, two additional considerations for understanding of the dynamic behavior of large truss space structures subjected to transient loadings will be introduced: the questions of how the energy imparted by the transient loads propagates throughout the lattice space structures and of how the spatial distribution of the system energy is influenced by the lattice design parameters and loading characteristics throughout the transient period. These additional considerations play important roles when the analyst is faced with vibration minimization tasks. For example, for the case of the envisioned paraboloid antenna truss structures, minimization of vibrations of the inner surface truss members is the design objective. In such cases, both the passive and active vibration control strategies are strongly influenced by the system energy shares of the core and the rear surface truss members relative to that of the inner surface members.

In order to demonstrate the importance of studying the energy distribution patterns, the transient response of a single tetrahedron cell isolated from the truss plate is studied when the cell is subjected to periodic excitations that approximate certain global truss-model vibration modes. Here, the practice of tailoring individual truss member stiffnesses to optimize the energy share of the core members is demonstrated. Second, the time history of the specific energy ratios of the core and surface members under bending and extensional deformations within the truss plate is analyzed. It is shown that even though the total average energy ratios do not undergo large fluctuations with time, those of the individual members do substantially, underscoring the significance of the interactions of the individual member motions with the global truss motions.

6.1. Single Tetrahedron Cell

A tetrahedral lattice cell is the smallest repeatable unit found in the lattice plate and comprises three members on each surface and six core members. This single cell was chosen for analysis because it is a representative unit of the entire truss structure, yet it is small enough to allow many numerical simulations to be performed in a relatively short time. As previously stated, the aim of this study is to obtain a quantitative idea as to how much influence the designer may be able to exert on the local member vibration energy levels. In particular, how much can the relative energy levels of the surface and the core members be varied by changes in member dynamic characteristics? In addition, since practical truss platform performance criteria call for a minimum of surface motion (as for paraboloid antenna, for instance), the core members become ideal candidates for application of passive or even active energy dissipation mechanisms. Accordingly, in the present study, the surface member slenderness ratio is held constant at s = 250 while the core member slenderness ratio is varied.

Figure 22 shows two truss regions from which the sample single cells are ispolated. These two locations are chosen as they exhibit relatively high energy concentrations of the core members in at least two of the lowest three modes determined in the free vibration analyses described in Section 2. Modal displacements from the first three global modes are extracted for these two regions and applied to the six joint nodes of the cell models as given by

$$\mathbf{q}_{app_i} = \mathbf{q}_i sin\ \omega_i t \tag{5}$$

where the $\mathbf{q}_i$ are modal displacements (elements of the i^{th} modal eigenvector), and ω_i are the discrete modal frequencies. All of the cell joints are modeled as ball joints in order to accurately capture the bending behavior of the core members. Each core member is discretized with two finite elements whereas only a single element is used to model each surface member. This discretization choice was made in order to use different moduli for the core and surface members to keep the critical time step as close

as possible. Accordingly, the core member material modulus is one quarter that of the surface member material.

Figures 23 and 24 show the specific member energy of the core and surface members as a function of the corresponding slenderness. Note the large energy shares of the core members when subjected to the second global mode excitation. Such large core member energy shares also appear in region 1 for the first and third modal excitations.

For the most part, the slenderness ratios at which the core members' energy shares are at maximum decrease with increasing excitation frequency. This relationship parallels the variation of member fundamental bending frequency, which increases as the slenderness ratio is lowered. Exceptions to this trend are found in the first and third mode results in region 2. The core member energy shares under first mode excitation are very small in region 2, indicating that little core member excitation is present in that region due to the first global mode. However, the core member energy share for the third mode excitation is at a maximum when the core and surface member slenderness ratios are equal. This result is indicative of a situation in which the dynamic loading of surface members increases as the core members are softened. In fact, this phenomenon is evident in all of the curves in Figures 23 and 24 as a lowering of the energy shares of the core members as s_c/s_s is increased slightly from a value of unity. Core member response to third mode excitation in region 2 is dominated by this effect.

Note that the large difference of the specific energy ratio at maximum and at minimum are indicative of sensitivity of the core members' relative energy concentration to changes in the slenderness ratio. This sensitivity is most pronounced in the second mode response curves, where a ratio of 1.7 occurs in region 1 and a ratio of 3.0 occurs in region 2.

6.2 Energy Propagation in the Truss Plate

Since it is evident that the member energy shares may be increased depending on the individual member's location within the lattice plate and on the primary excitations experienced by the member, it is desireable to predict those locations at which the dynamic characteristics of certain members can be tailored for a reduction in undesireable transient motions of the truss plate. To accomplish this, the energy concentration patterns are mapped onto the lattice plate. The maps made in a time sequence show the transfer of energy among members as the truss plate undergoes transient motions.

Spatial distributions of the deformation energy levels of the individual members are most easily communicated by color-coding the individual members according to their relative energy shares on the structural model. This technique is known as color contour plotting. In analysis of energy levels from the transient response simulations, a total of eight colors are used to represent the variations of member specific energies. The colors are chosen based on the minimum and maximum specific strain energy levels present in the truss plate for the displayed timestep. As such, the color scale is a relative rather than an absolute scale.

A time sequence of nine specific energy contour plots is shown in Figure 25. These plots were taken from the first .036 sec. of response of a quarter-size truss plate model subjected to an initial out-of-plane impulse at the lower left corner. The color scale at the right of each frame represents variations of the specific strain energy from the minumum (dark blue) through the maximum (white) level in that frame. Thus, the sequence of plots shows the propagation of strain energy through the truss plate. Of note in this display are the preferred directions of energy transfer through the plate and the effects of free-edge reflections of the travelling energy.

A detailed examination of the member deflections associated with this initial energy propagation reveals the primary mechanism of energy transfer to be axial stress waves travelling through the truss members. Specifically, energy is distributed throughout the truss by transfer among the the plate surface members. The preferred direction of energy transfer in the surface truss members is among the members of the same directional alignment. Thus, energy propagates along members aligned with the horizontal direction of the frame (x-direction) and along members aligned with the 60°-to-horizontal direction from the point of initial excitation. Energy exchange between the upper and lower surface truss members occurs through local groups of the core members.

Although some spreading of energy occurs at truss joints, the transfer of energy to members not aligned with the primary directions of propagation occurs mostly through reflection of the stress waves at the free edges of the truss plate. This effect can be seen most dramatically in the last few frames of Fig. 25. The propagation of the deflection wave also causes the core members aligned with the propagation path to be loaded. As can be seen from the last few frames of Fig. 25, the core members near a free edge can acquire a large energy share as the initial wave is reflected.

Vibration energy due to member bending also propagates in the same manner as described above. Since bending frequencies are $2 \sim 3$ orders of magnitude lower than axial vibration frequencies, these motions do not appear with significance in the very early time energy distributions. However, a close look at the energy exchange mechanisms of the truss members during the first observable global vibration cycle reveals that adjacent members do exchange their bending energy. In the case of high-slenderness members, the bending energy exchange can account for sizeable fluctuations in vibration energy levels of a truss member. Furthermore, as the member slenderness ratio is increased, nonlinear effects of compressive loadings may play an important role in decreasing the effective axial frequency of the members, with the result that primary stress wave energy propagation would occur at a rate comparable to bending energy exchange in truss members undergoing compression.

6.3 Energy Distribution Among Truss Plate Members

As discussed in Sections 2 and 3, the bending behavior of individual truss members is a *local dynamic* phenomenon. The influence of this local effect can be assessed by

measuring the energy stored in the truss members due to bending as a fraction of the total energy, or equivalently the average ratio of member bending energy to member extensional energy. This ratio is defined as

$$\bar{R} = \frac{Specific\ Bending\ Energy}{Specific\ Extensional\ Energy}$$

$$\bar{R}_{avg} = \frac{Average\ Specific\ Bending\ Energy}{Average\ Specific\ Extensional\ Energy} \tag{6}$$

$$= \frac{1}{m}\sum_{m}\frac{1}{2l}\left\{\frac{\frac{I}{A}\int_{l_i}(\kappa_y^2+\kappa_z^2)dx}{\int_{l_i}\epsilon_x^2 dx}\right\}$$

where m is the number of surface or core members in the truss model. Figures 26 and 27 show the history of the average ratio of member specific bending energy to extensional energy for the transient cases of $s = 250$ and $s = 600$.

It is interesting to note that individual members may undergo a sizeable fluctuation in $\bar{R}$ over time. Figure 28 shows the time history of $\bar{R}$ for a single core member. The two very large peaks in this figure have values of the order of 10.0. Quite naturally, the magnitude of such variation depends on the particular location and loading of the individual member. The aggregate behavior of all of the truss members of a particular class (i.e. truss core or surface members), as depicted in Figs. 26 and 27, exhibits a much smaller variation.

As mentioned previously, nonlinear effects due to member compression may be significant, especially in truss structures composed of members of high slenderness ratio. To account for member nonlinear behavior in truss plate energy distributions, a revised method for calculating member specific energies is suggested. Briefly, if axial stiffness is reduced due to imperfection sensitivity according to Eq. (1), then specific extensional energy should be reduced by the factor κ as well.

$$\bar{U}_{e_{NL}} = \kappa \bar{U}_{extension} \tag{7}$$

Further, to keep the total specific energy of the member constant, and noting that bending deflections will be increased due to compression, the bending energy must also be modified.

$$\bar{U}_{b_{NL}} = \bar{U}_{bending} + (1-\kappa)\bar{U}_{extension} \tag{8}$$

Because the total energy level within a member will probably decrease with significant member nonlinearity, the ratio of $\bar{U}_{b_{NL}}$ to $\bar{U}_{b_{NL}}$ represents an upper bound of $\bar{R}$ for imperfection sensitive members subjected to compressive loads.

When this approximation is used, the average bending energy content increases dramatically. Figures 29 and 30 show the upper bound approximation for $\bar{R}_{avg}$. Comparison of these Figures with Figs. 26 and 27 reveal the effect of the inclusion of member imperfection sensitivity on the energy distribution within the truss plate, namely, to increase the bending energy share of the members. In particular, the bending energy share for members of high slenderness increases much more than that for members of low slenderness. Thus, when members deform in compression, the higher the slenderness ratio, the more the member energy is likely to be in member bending modes.

7. Major Results and Discussions

In this report, the study of the dynamic behavior of lattice truss plates has been conducted based on finite element models in which the truss members are assumed to be slender beams. The reason for such discrete beam modeling was to investigate the influence of the local dynamic characteristics of the individual members on the global transient responses of the truss plate. The present study offers the following results.

- In general, the transient responses of the lattice truss plate considered during the present study indicate that the responses consist of many frequency components at significant amplitudes and over a wide frequency band. This can be readily seen in deflection time histories like those presented in Section 4. The number of excited components and the amplitudes associated with them have been found to depend strongly on the character of the applied excitations and truss member properties.

- A close examination of the transient responses reveals that the local member dynamics significantly influence the overall dynamic behavior of lattice truss plates. Sizeable variations in primary global mode period and in higher mode amplitudes, occurring as a result of changing the slenderness ratio of the truss members, are examples of this influence. As such, overall truss motions cannot necessarily be adequately described in terms of classical global modal analyses; the member dynamics must be considered in the transient response behavior of lattice truss structures. Therefore, it is concluded that the continuum modeling methods [5,6] which have been advocated for describing the global truss dynamic characteristics may not adequately account for the dynamics of the individual truss members and/or the global transient dynamics unless extensive refinements are introduced from the outset.

- It is recommended that, if one is to exploit the inherently discrete character of lattice truss structures to the fullest advantage, variations of the dynamic properties of the individual truss members present an effective design consideration. As observed in Section 6.1, large variations of the member dynamic response are possible , even within a relatively constant global vibration environment, by selective variation of truss member slenderness ratio (cf. Figs. 23, 24).

The above results have direct bearings on the passive and active control strategies, which can be stated as follows.

- Undersirable global transient responses could either be isolated to selected local regions where they could be controlled by active means, or, in some cases, reduced to an insignificant level. This may be accomplished by design modifications of individual members.
- Wideband control requirements in active vibration controls may be significantly eased by customizing the control strategies to a certain area of the lattice in which significant high-frequency vibrations occur in a reliably predictable manner.
- Energy dissipation devices may be placed in the most advantageous locations for each individual mode. This leads to a lattice with a globally nonuniform structure which may also be advantageous for tailoring global frequencies and/or mode shapes. The effectiveness of these devices would depend on the specific design parameters of the core and surface members and especially on their integration into the lattice truss plate.

It should be noted that the preceding results and observations are based on linear analyses. In reality, however, because the truss members under consideration are designed to have their slenderness ratios well in excess of 250, it is very much likely that the truss plate will exhibit significant nonlinear responses to conceivable transient loadings. Future studies, therefore, must adequately account for the effects of nonlinear behavior and the extent of applicability of the present results must be carefully scrutinized by more realistic nonlinear analysis.

Another assumption introduced in the present study is the modeling of truss joints as ideal ball joints. In practice, the joints constructed will probably have constraints on bending in one or more direction. Also, real joints exhibit some friction and, although the magnitude of friction forces may be small, the members will also be very light and will no doubt be influenced by forces induced by the joints. This aspect, too, must be evaluated in future studies by incorporating more realistic joint models.

Acknowledgements

The work presented herein has been supported by Air Force Office of Scientific Research under Contract F49620-83-C-0018. The authors wish to thank Dr. A. K. Amos for his interest in the present work and for his encouragement throughout the present study.

References

1. Wah, T., "Vibration of Cylindrical Gridwork Shells," *AIAA J.*, 3, Aug. 1965.

2. Anderson, M. S., "Vibration of Prestressed Periodic Lattice Structures," AIAA Dynamics Specialists Conf., Atlanta, Georgia, April 1981, AIAA Paper No. 81-0620

3. Park, K. C., and Winget, J. M., "A Structural Approach for Vibration Control of Large Space Truss Structures," Lockheed Palo Alto Research Laboratory, Report LMSC-D878966, September 1982.

4. Renton, J. D., "On the Grid-Framework Analogy for Plates," *J. Mech. Phys. Solids*, 1965, 13, pp. 413-420.

5. Noor, A. K., Anderson, M. S., and Greene, W. H., "Continuum Models for Beam- and Platelike Lattice Structures," *AIAA J.*, 16, Dec. 1978, 1219-1228.

6. Nayfeh, A. H., and Hefzy. M. S., "Continuum Modeling of the Mechanical and Thermal Behavior of Discrete Large Structures," *AIAA J.*, 16, Aug. 1978, 779-787.

7. Park, K. C., and Underwood, P. G., "A Variable-Step Central Difference Method for Structural Dynamics Analysis," *Comp. Meth. App. Mech. Engr.*, 22 (1980), 241-258.

8. Underwood, P. G., and Park, K. C., " STINT/CD: A Stand-Alone Explicit Time Integration Package for Structural Dynamics Analysis," *Int. J. Num. Meth. Engr.*, 17 (1981), 1285-1312

9. Bathe, K. J., *Finite Element Porcedures in Engineering Analysis*, (Chapter 9), Prentice Hall, Englewood Cliffs, New Jersey, 1982.

10. Meirovitch, L., *Elements of Vibration Analysis*, McGraw-Hill, New York, 1975.

Appendix

Modulus Modification due to Member Imperfection Sensitivity

An expression describing the effective reduction of the axial stiffness of a very slender truss member due to presence of small imperfections is derived below. This stiffness modification, as appearing in Equation (1), provides a linearized approximation of reduction of axial stiffness due to small compressive loadings or small end-shortening displacements.

The imperfect member is postulated to have an initial transverse displacement according to

$$w_{initial} = w_0 \sin \frac{\pi x}{L} \tag{A.1}$$

where w_0 is the magnitude of the imperfection at midspan ($x = L/2$). Under a compressive loading P applied at each end, the bending moment due to the initial transverse displacement is

$$M(x) = P w_0 \sin \frac{\pi x}{L}. \tag{A.2}$$

Using the stress-moment relation from simple beam theory and relating the resulting axial stress due to bending to the compressive strain in the member provides an expression for the axial strain in terms of the applied load P.

$$\epsilon_x = \frac{du}{dx} = \frac{P}{EI} w_{initial} \tag{A.3}$$

Substituting from Equation (A.1) and integrating once with respect to x yields

$$u = \frac{1}{2} \frac{PL}{EI} w_0^2. \tag{A.4}$$

The total end-shortening due to the compressive loading is thus the sum of that due to the elastic axial straining and that described in Equation (A.4).

$$\begin{aligned} \delta &= \frac{PL}{AE} + \frac{1}{2} \frac{PL}{EI} w_0^2 \\ &= \frac{PL}{AE} \left[1 + \frac{1}{2} w_0^2 \frac{A}{I} \right] \end{aligned} \tag{A.5}$$

Setting the imperfection parameter α equal to the quantity w_0/L, Equation (A.5) becomes

$$\delta = \frac{PL}{AE}\left[1 + .5\frac{\alpha^2 L^2 A}{I}\right]$$
$$= \frac{PL}{AE}\left[1 + .5(\alpha s)^2\right] \qquad (A.6)$$

Thus, the κ of Equation (1) is defined as the modifying factor to the conventional linear axial stiffness, determined by the ratio of the applied compressive loading P to the total end-shortening δ.

$$\frac{P}{\delta} = \frac{EA}{L}\left[\frac{1}{1 + .5(\alpha s)^2}\right]$$
$$= \kappa\frac{EA}{L} \qquad (A.7)$$
$$= \frac{\bar{E}A}{L}$$

The validity of this linearized approximation for member imperfection sensitivity was tested using two-node Hermitian cubic beam finite elements in the STAGS finite element code. End-shortening displacements were applied to imperfect beam member models of various slenderness ratios and the specific strain energy, as defined in Equation (2), was calculated from the resulting displacements. Using the calculated specific energy from the lowest slenderness ratio test as a basis, specific energies of members of higher slenderness ratio were normalized and plotted vs. relative slenderness. This plot appears in Figure A.1 along with the prediction obtained using the linearized approximation of Equation (A.6).

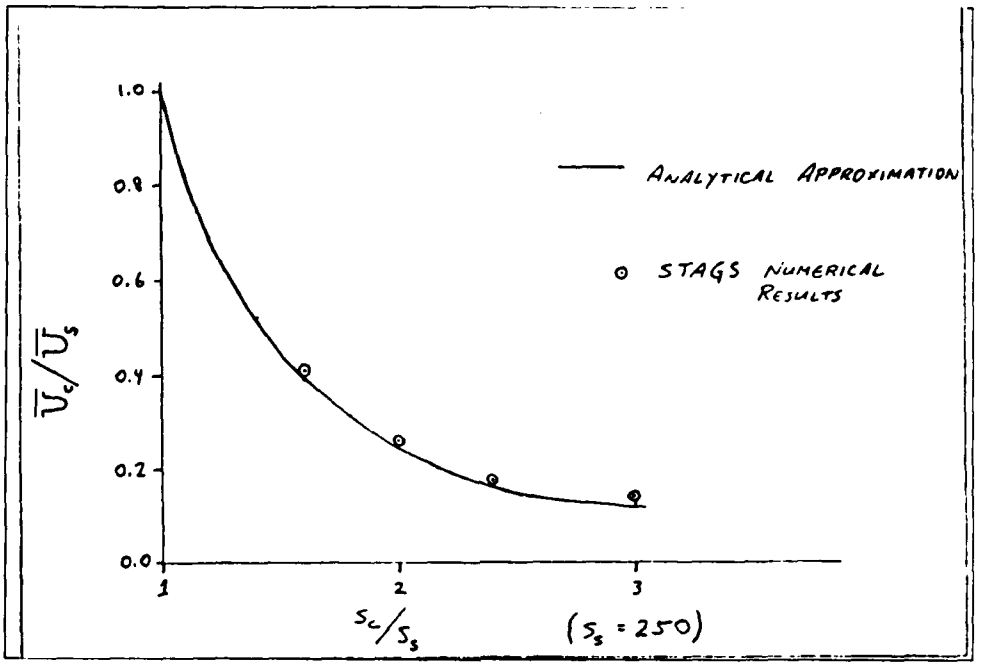

Figure A.1. Analytical/Numerical Evaluation of Approximation

The very good agreement of analytical and numerical results apparent in Figure A.1 is indicative of the correct application of the approximation. In particular, one should note that *relative* levels of strain energy of imperfect members undergoing comparable axial deformations are predicted accurately by the approximation.

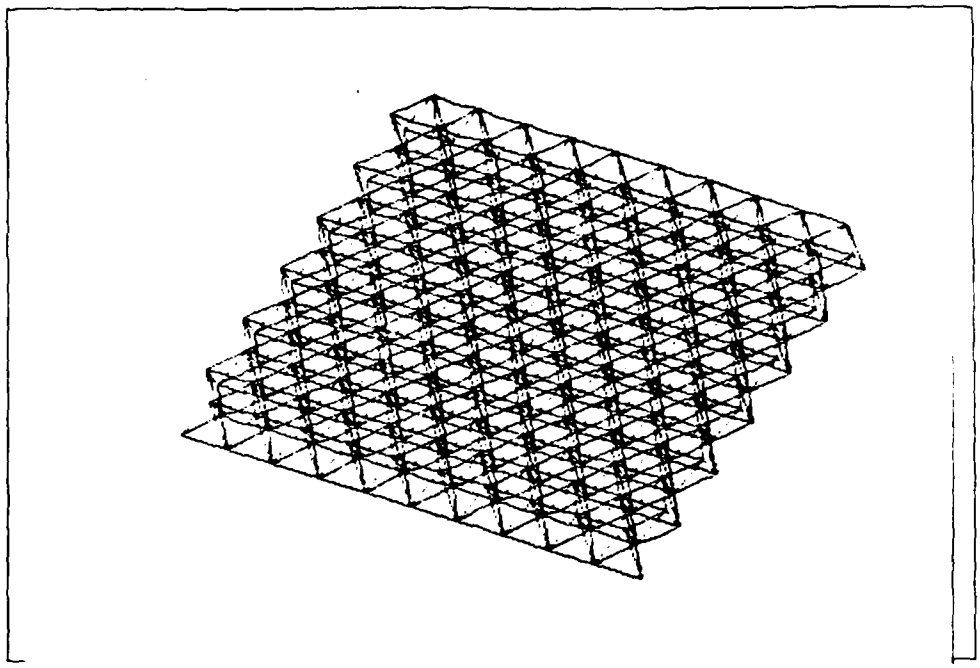

Figure 1. Tetrahedral Truss Plate Model

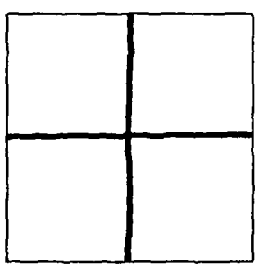

$f_{\lambda_1} = 2.996$ Hz.

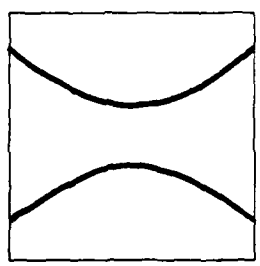

$f_{\lambda_2} = 4.129$ Hz.

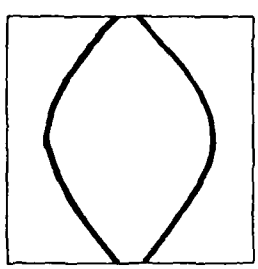

$f_{\lambda_3} = 5.613$ Hz.

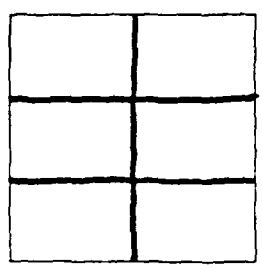

$f_{\lambda_4} = 6.810$ Hz.

Figure 2. Vibration Nodal Lines and Frequencies of the Truss Plate

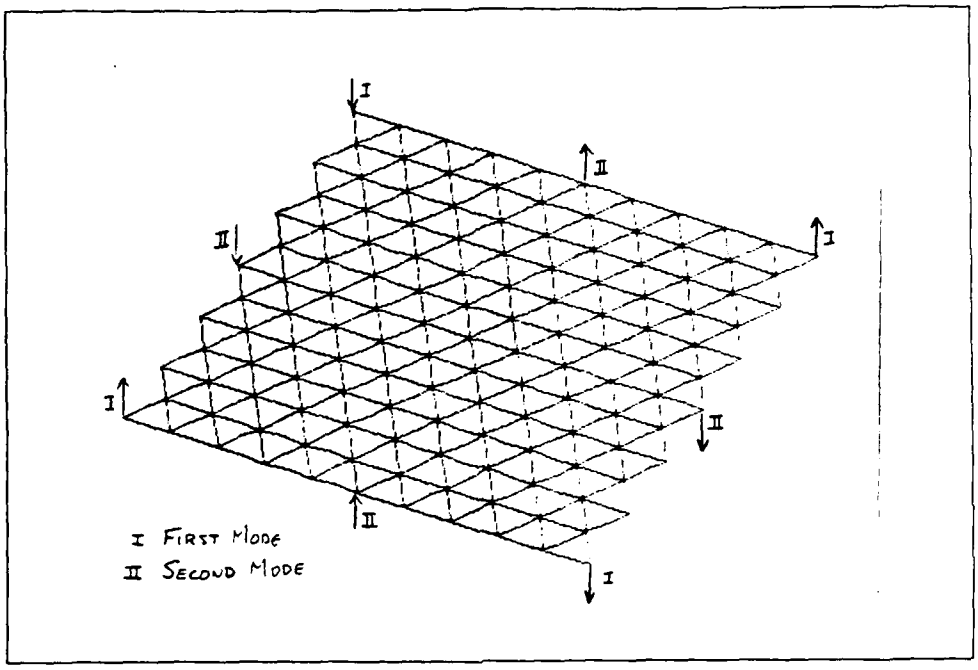

Figure 3. Impulse Loading Locations
(Core and upper surface members removed for clarity)

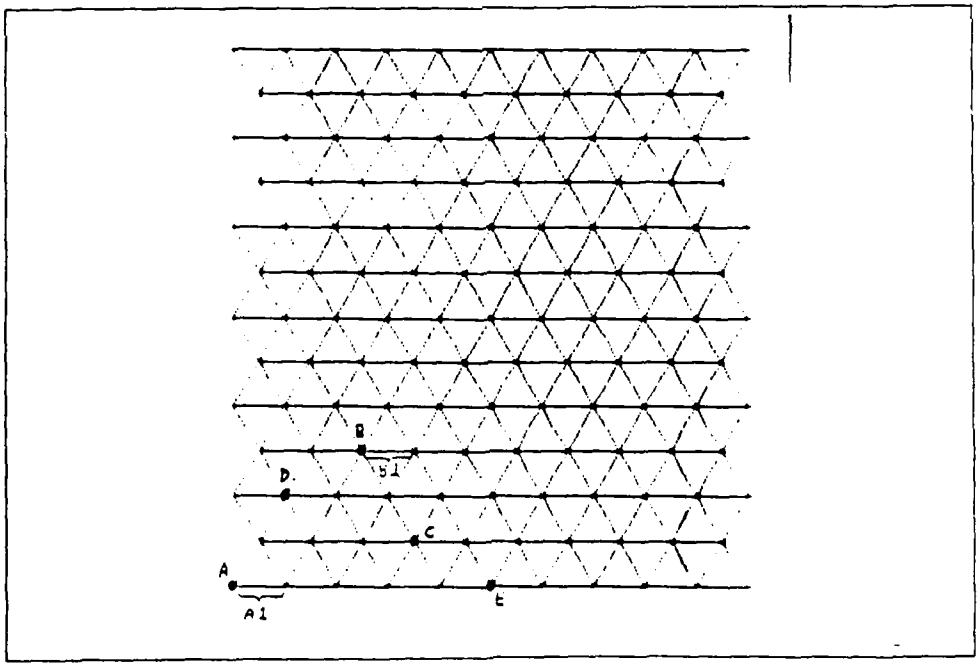

Figure 4. Response Sample Locations
(Core and upper surface members removed for clarity)

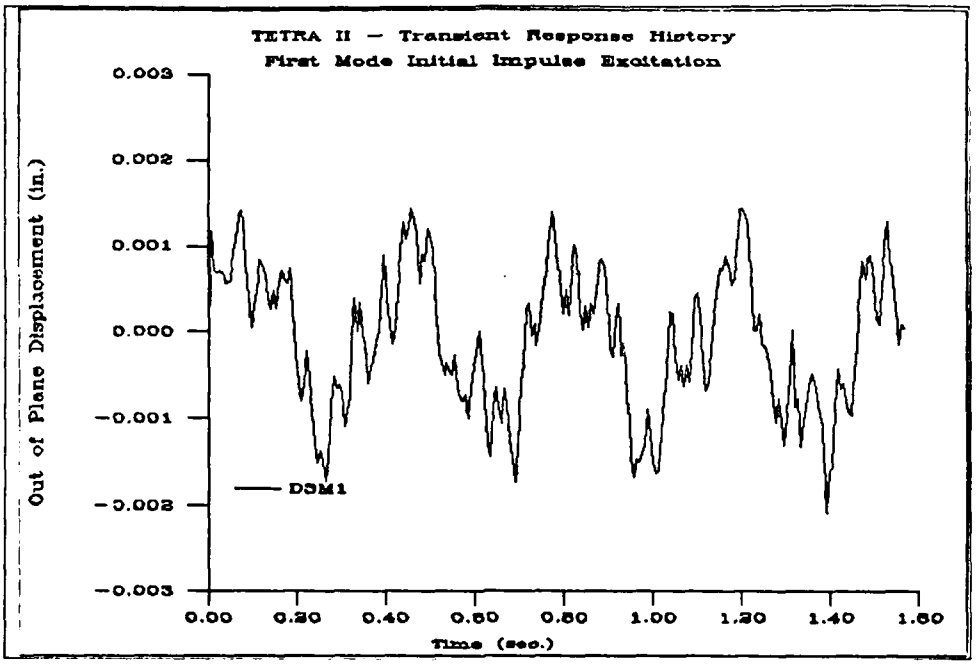

Figure 5. Response at Truss Joint A ($s = 250$)

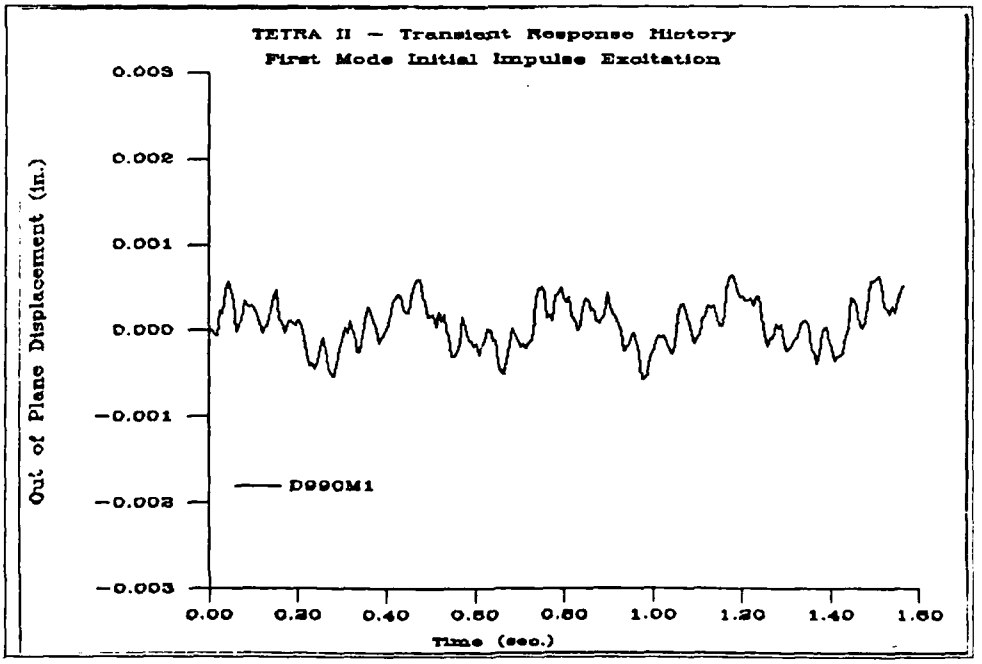

Figure 6. Response at Truss Joint B ($s = 250$)

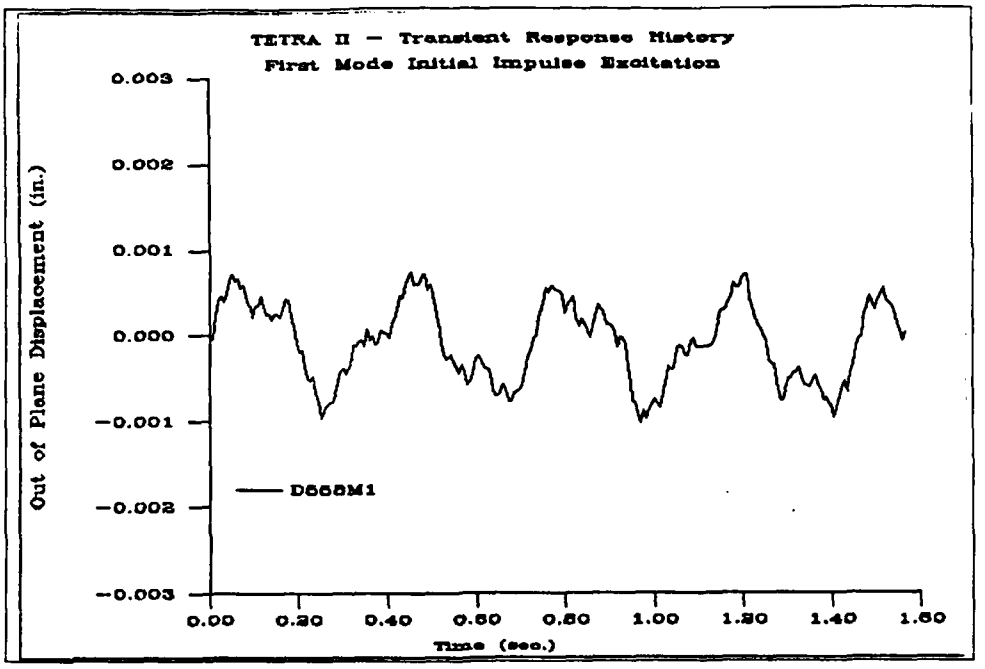

Figure 7. Response at Truss Joint D ($s = 250$)

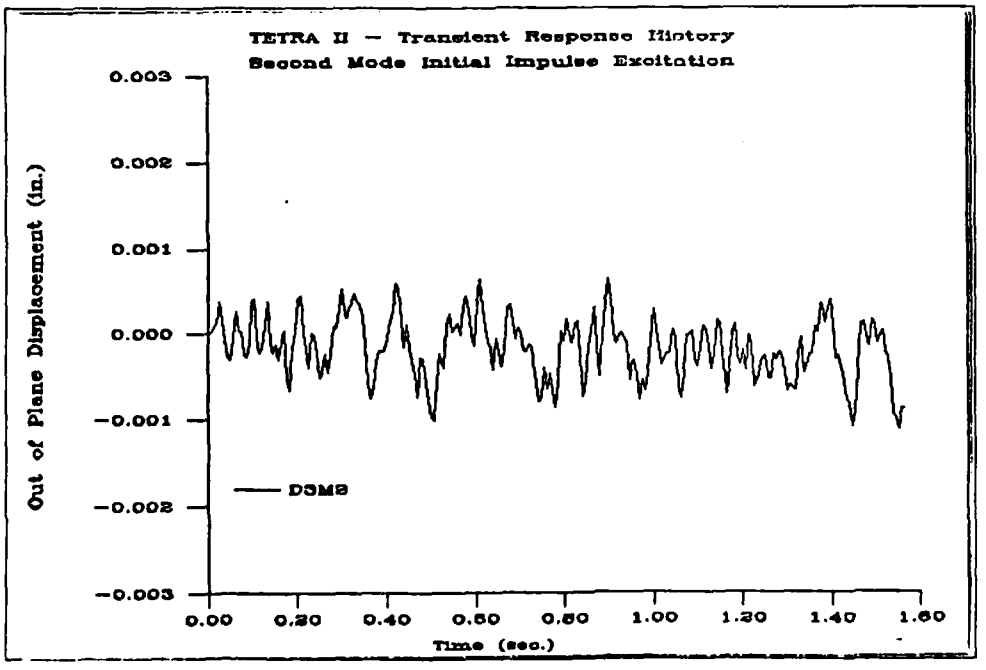

Figure 8. Response at Truss Joint A ($s = 250$)
(*Second Mode Excitation*)

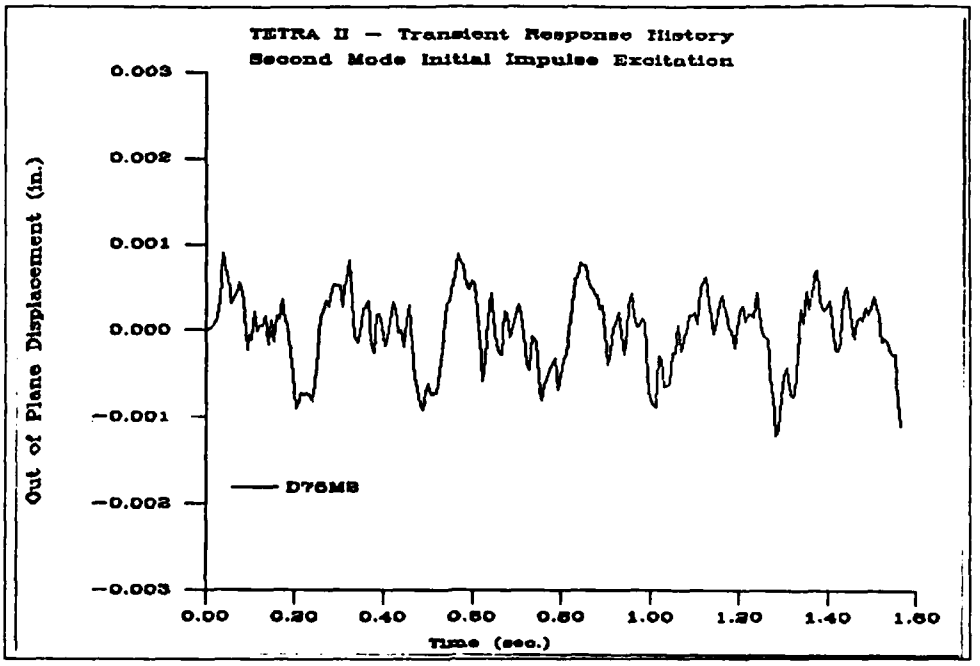

Figure 9. Response at Truss Joint E ($s = 250$)
(*Second Mode Excitation*)

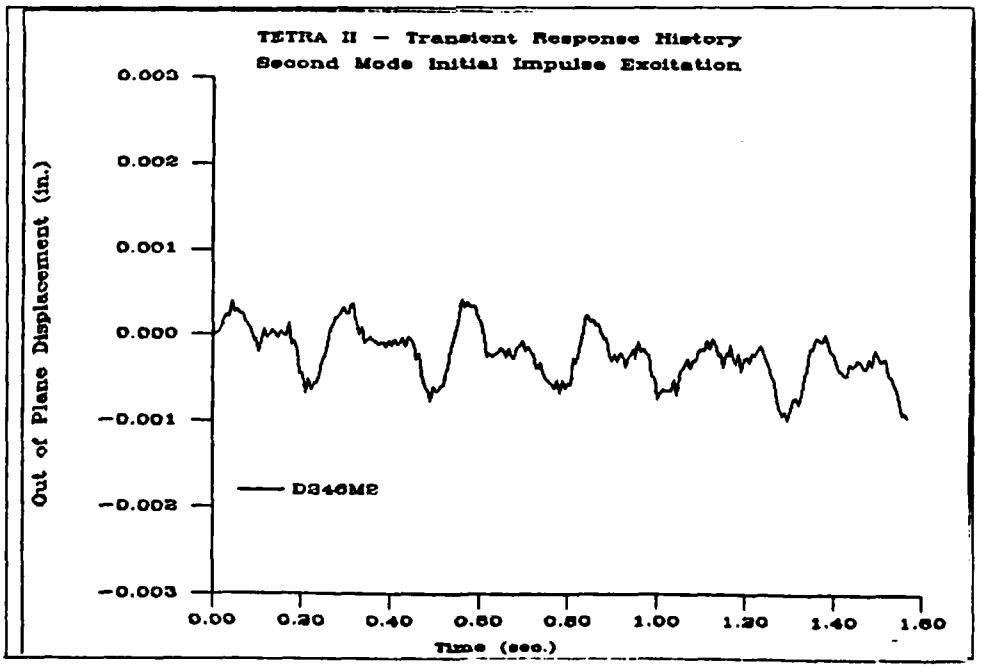

Figure 10. Response at Truss Joint C ($s = 250$)
(*Second Mode Excitation*)

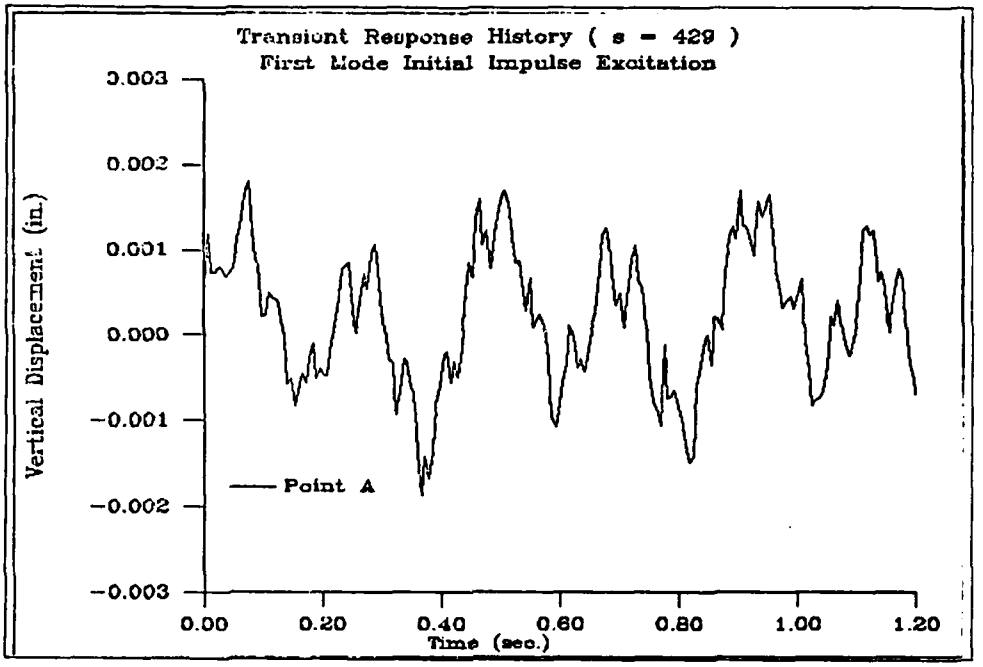

Figure 11. Response at Truss Joint A ($s = 450$)

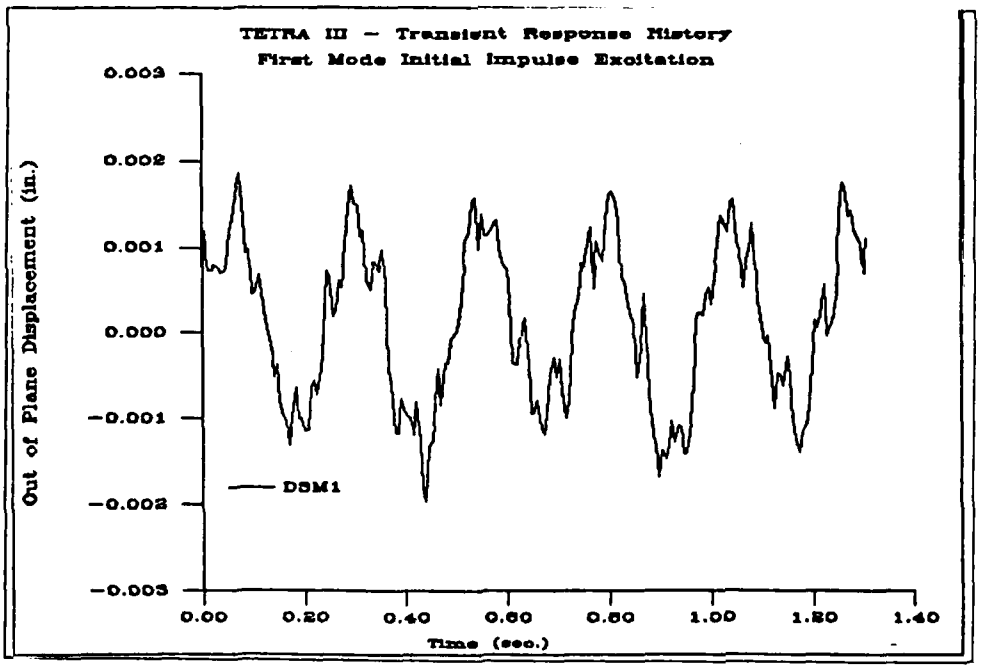

Figure 12. Response at Truss Joint A ($s = 600$)

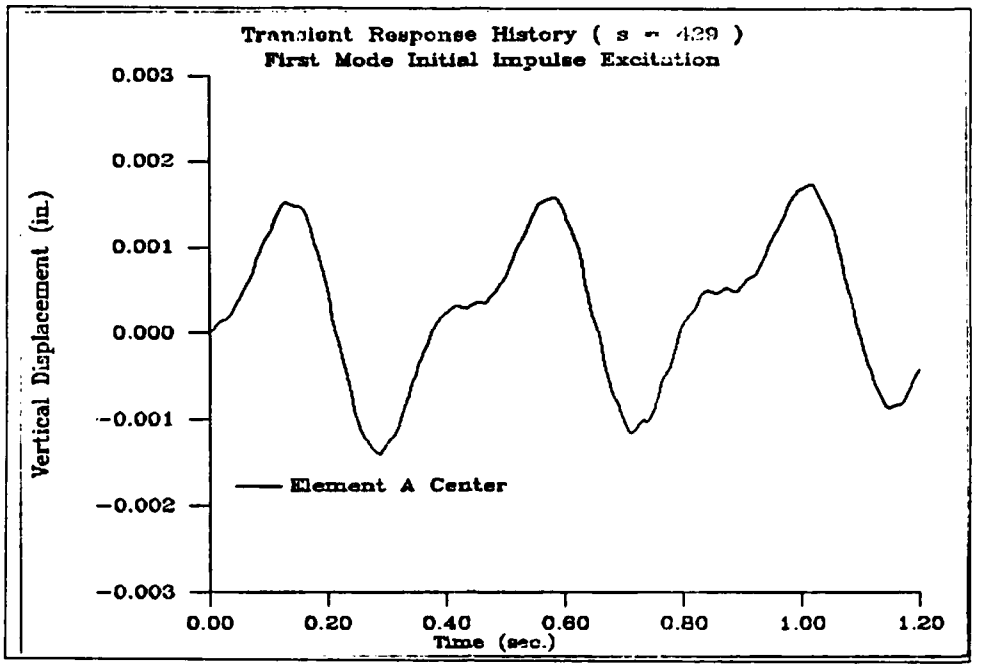

Figure 13. Response at Center of Member A1 ($s = 429$)

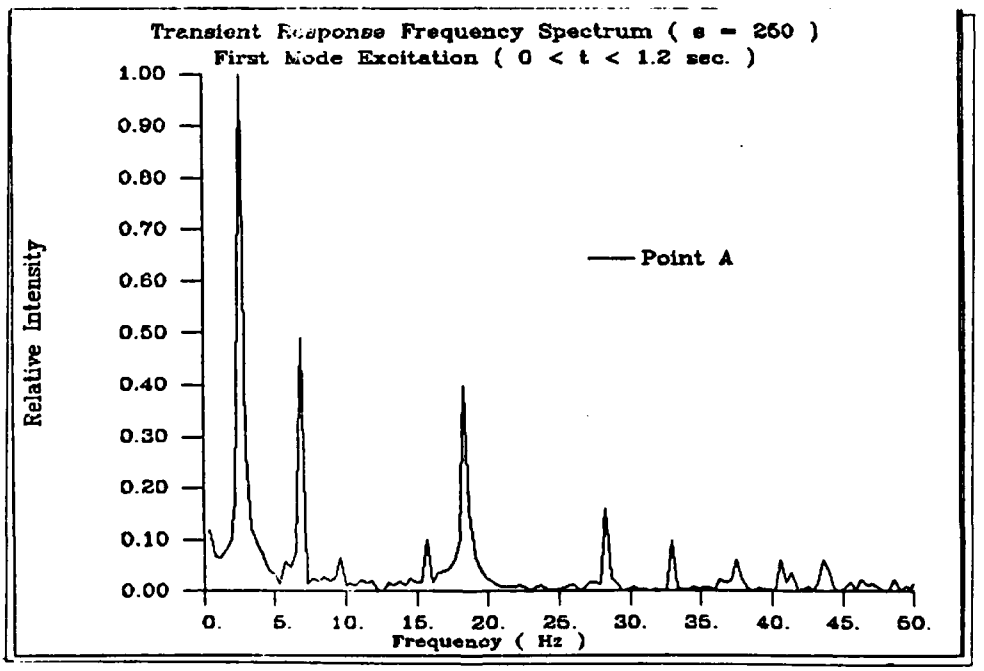

Figure 14. Fourier Spectrum at Truss Joint A ($s = 250$)

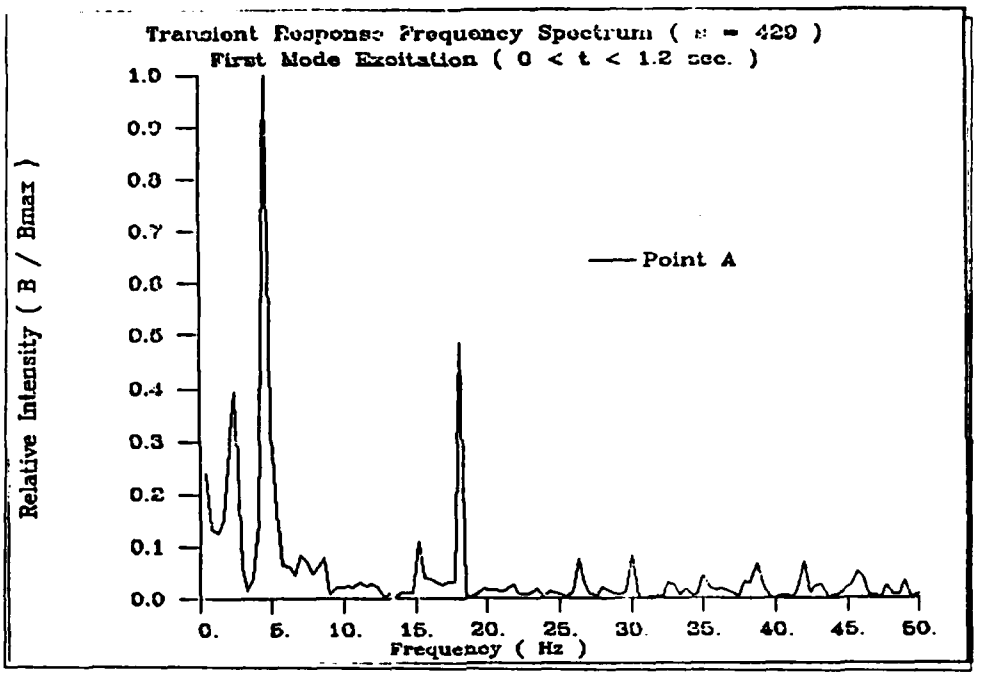

Figure 15. Fourier Spectrum at Truss Joint A ($s = 429$)

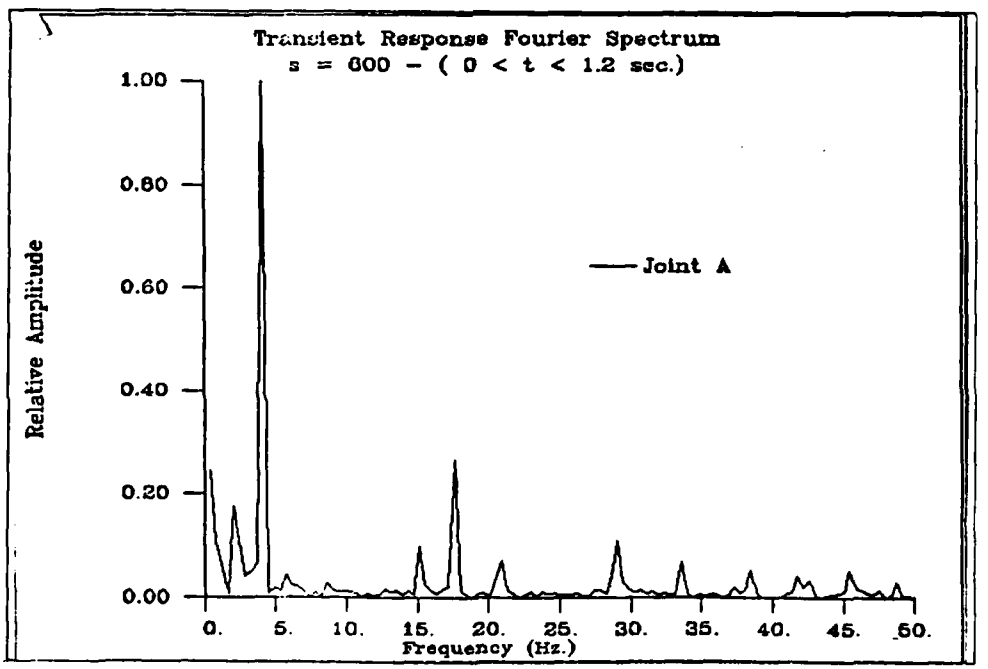

Figure 16. Fourier Spectrum at Truss Joint A ($s = 600$)

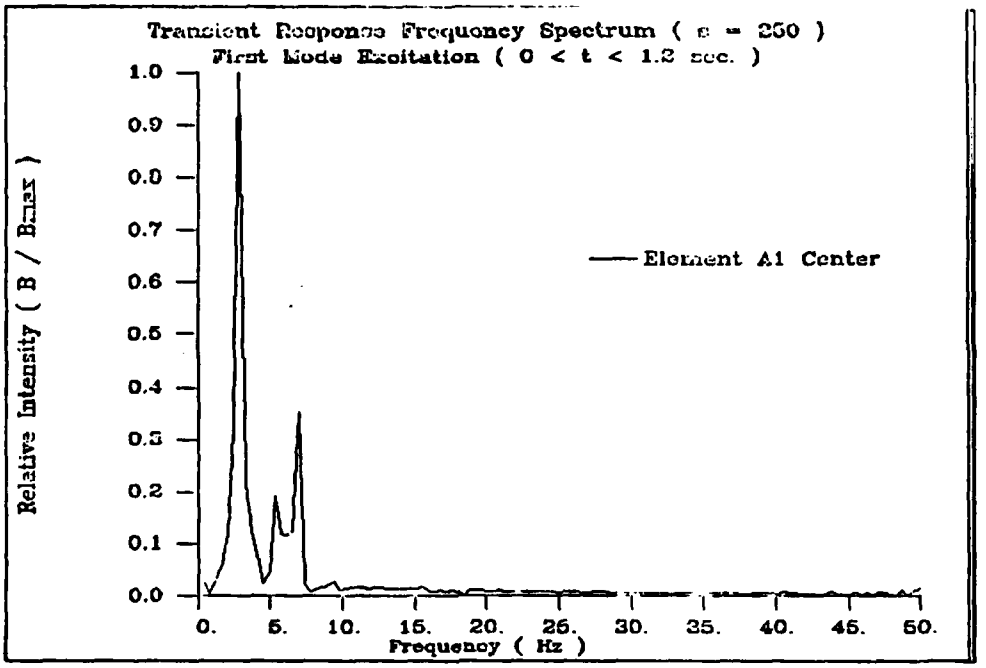

Figure 17. Fourier Spectrum at Center of Member A1 ($s = 250$)

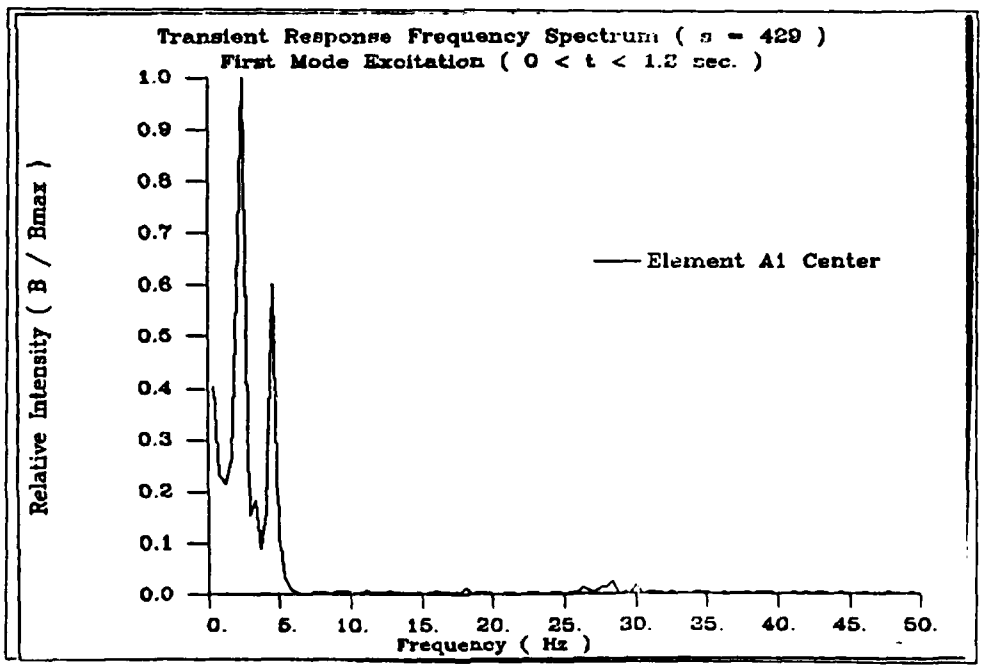

Figure 18. Fourier Spectrum at Center of Member A1 ($s = 429$)

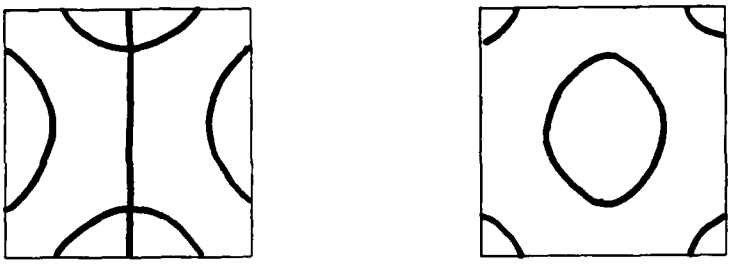

(a) 17.68 Hz. Mode (b) 18.99 Hz. Mode

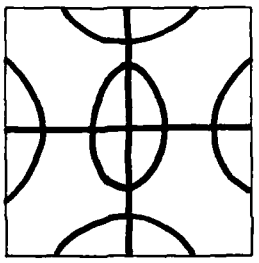

(c) Combined Mode

Figure 19. Superposition of High Frequency Truss Modes

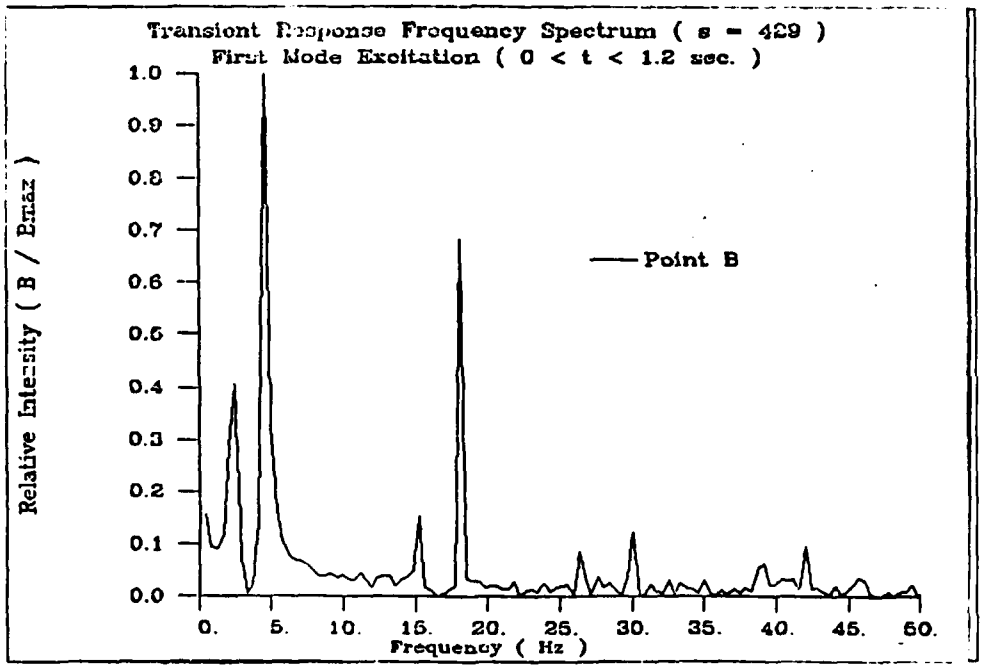

Figure 20. Fourier Spectrum at Truss Joint B ($s = 429$)

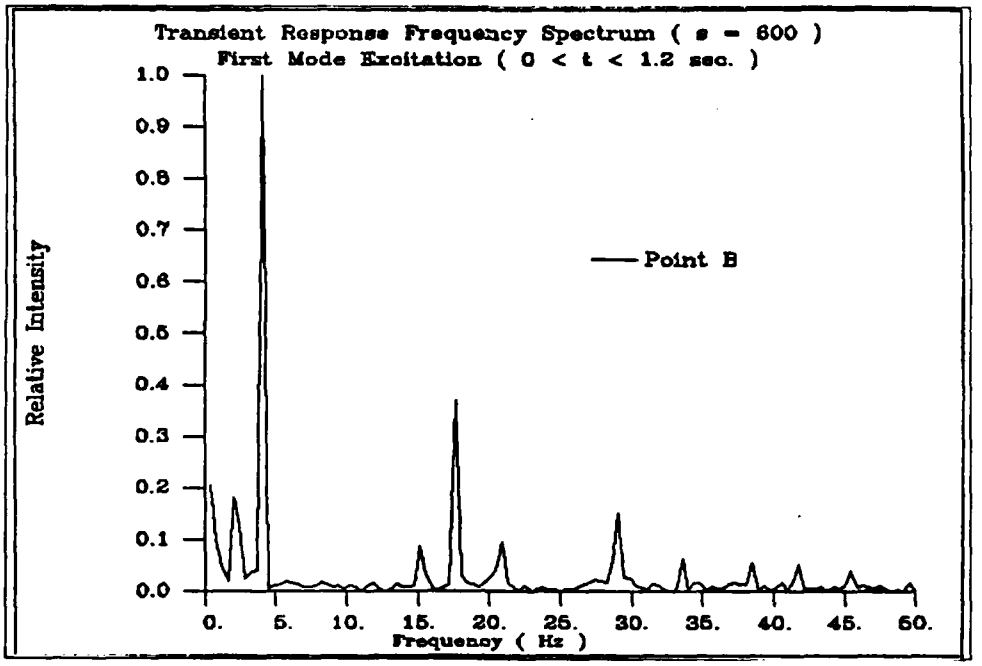

Figure 21. Fourier Spectrum at Truss Joint B ($s = 600$)

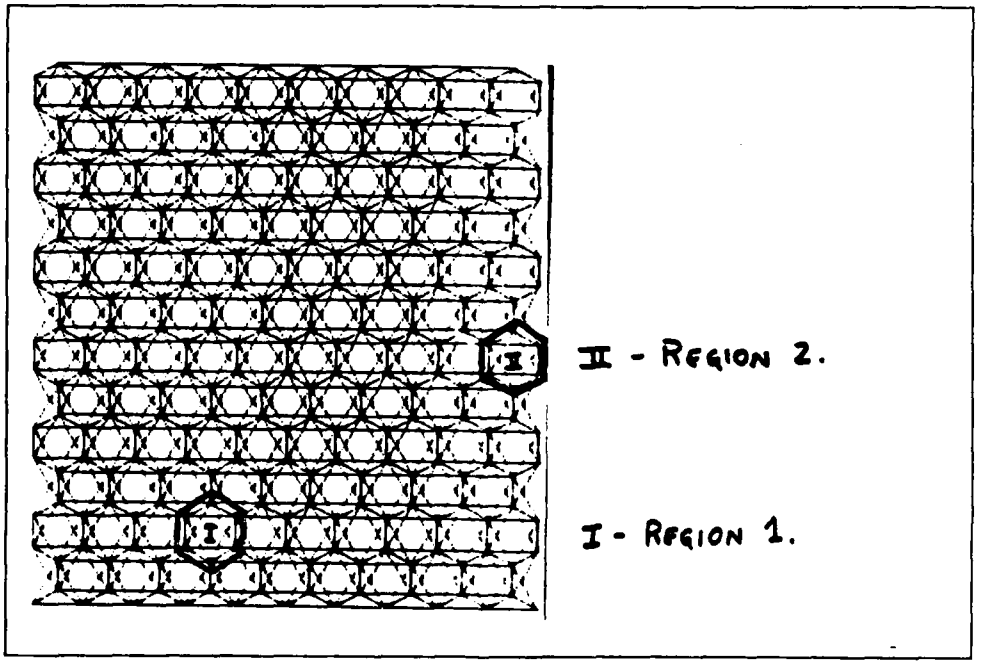

Figure 22. Single Cell Locations

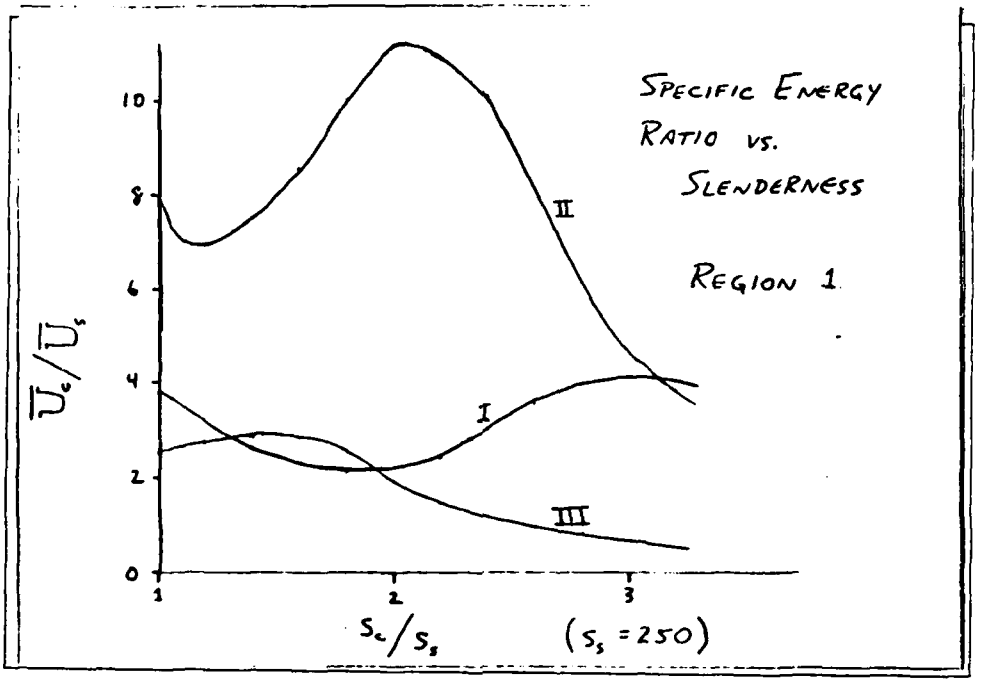

Figure 23. Cell Member Specific Energy Ratios - Region 1

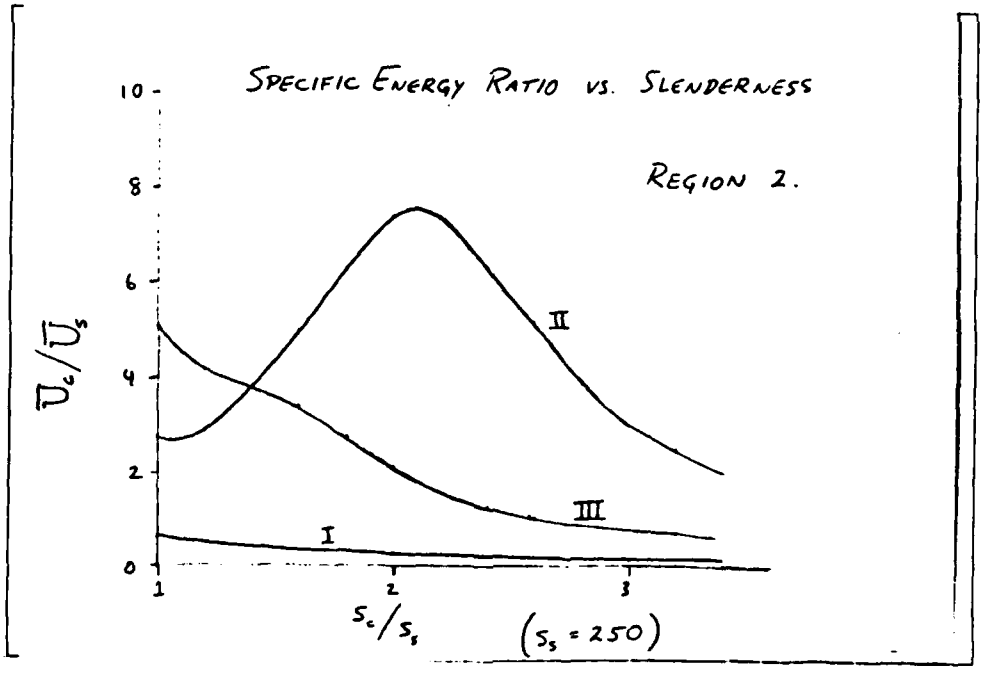

Figure 24. Cell Member Specific Energy Ratios - Region 2

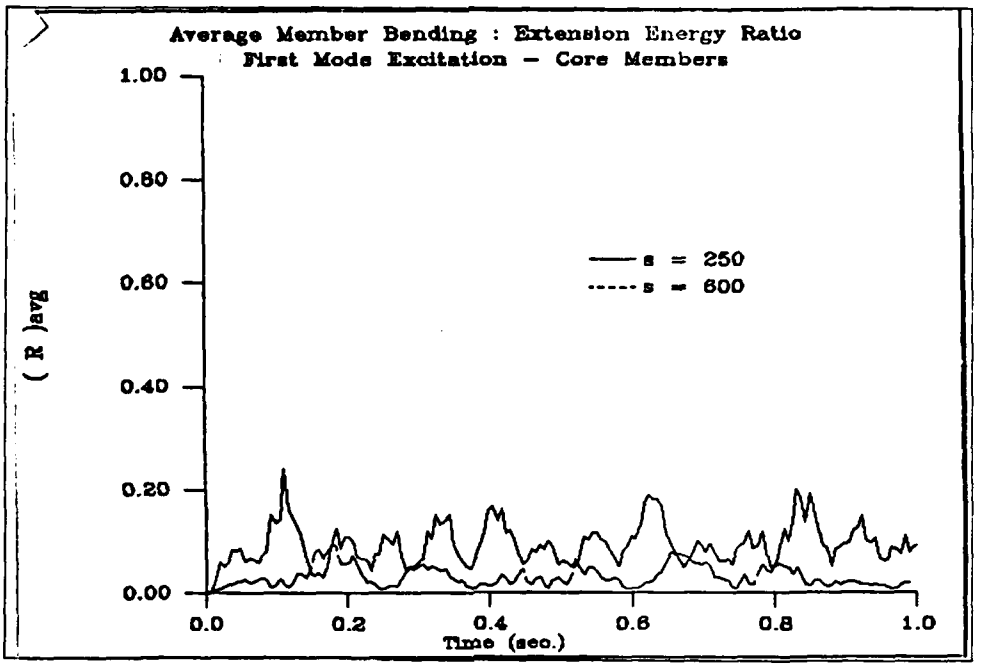

Figure 26. Core Member Specific Energy Ratio

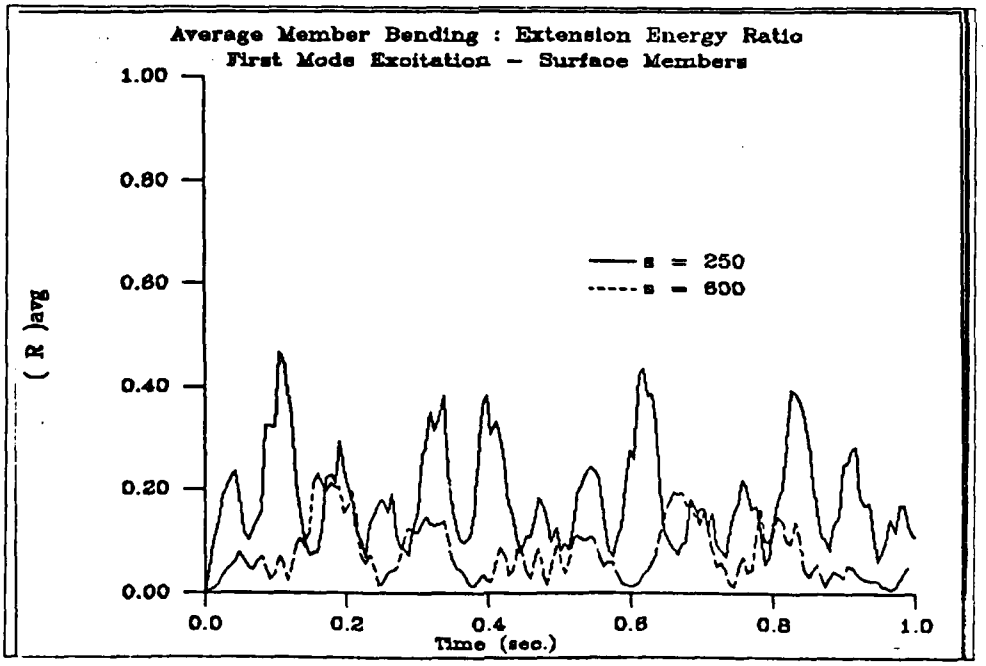

Figure 27. Surface Member Specific Energy Ratio

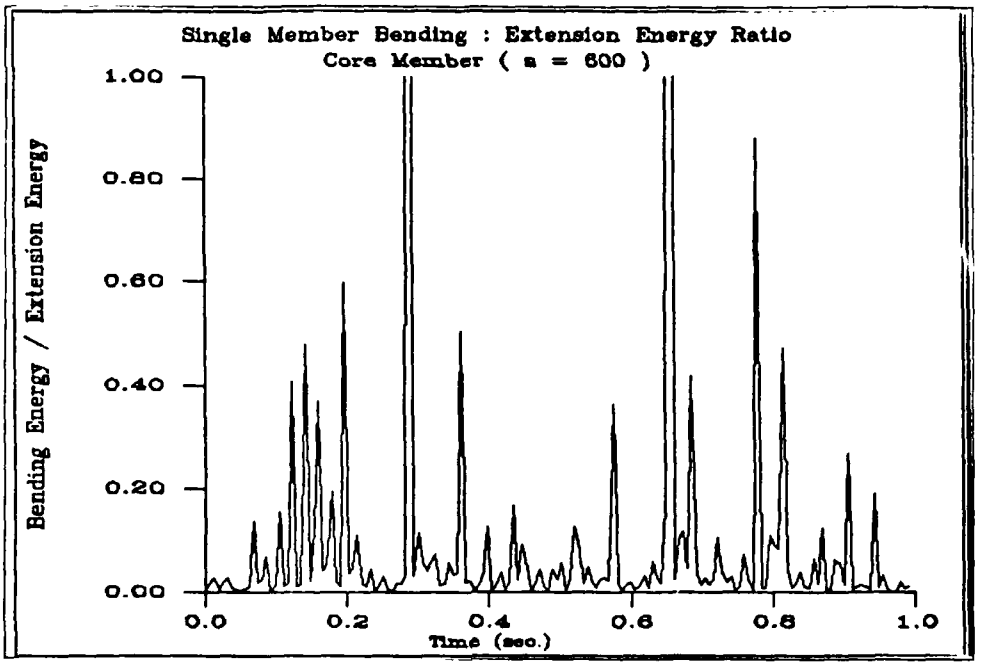

Figure 28. Single Core Member Specific Energy Ratio

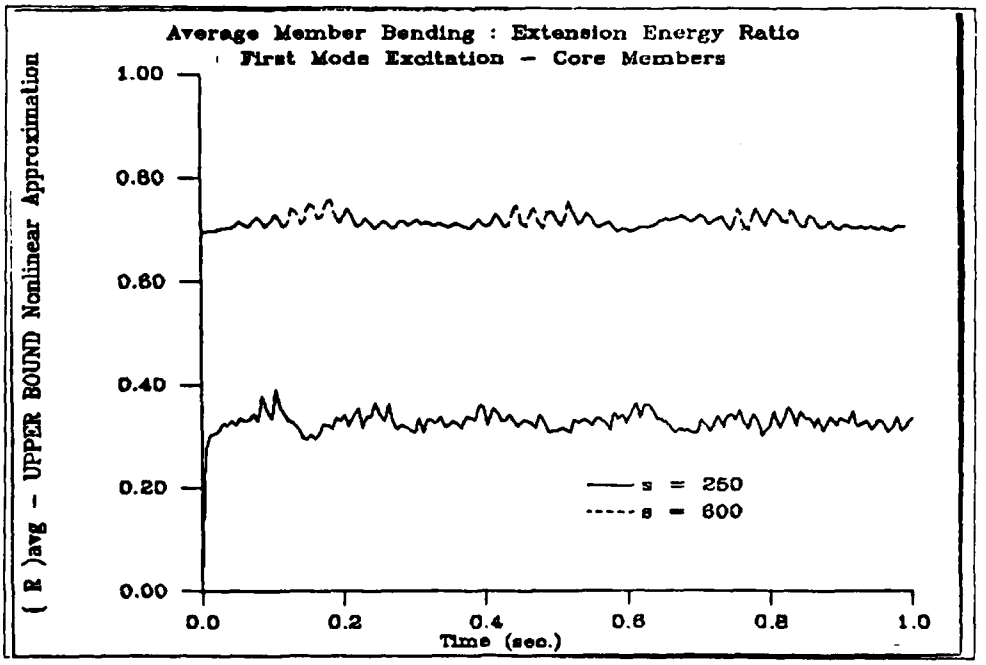

Figure 29. Upper Bound for Core Member $\bar{R}_{avg}$

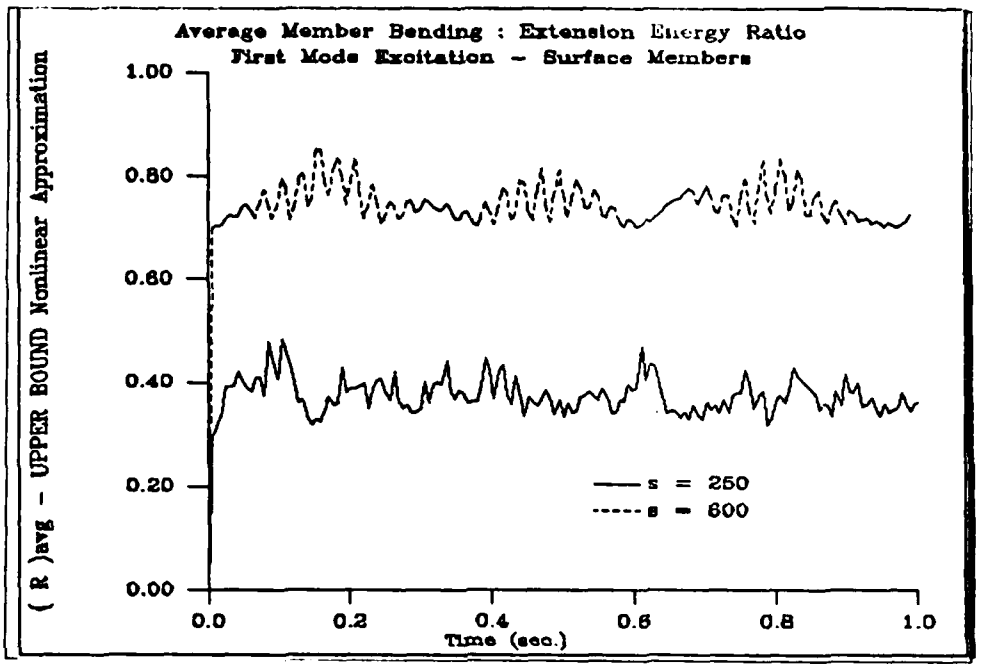

Figure 30. Upper Bound for Surface Member $\bar{R}_{avg}$

END

1-87

DTIC